



The Concept, Deposition Routes, and Applications of Superhydrophobic Surfaces – Review

Mona Hassan^{a*}, Zeinab Abdel Hamid^a, Sayed S. Abd El Rehim^b, Ahmed Ibrahim^c,
Maamoun A. Maamoun^a



CrossMark

^a Central Metallurgical Research and Development Institute (CMRDI), Cairo, Egypt

^b Chemistry department, Faculty of science, Ain shams university, Cairo, Egypt

^c Mechanical Engineering Department, Farmingdale State College, Farmingdale, NY 11735, USA

Abstract

The superhydrophobic surface (SHS) is the surface with a high apparent contact angle ($> 150^\circ$), low hysteresis in the contact angle ($< 10^\circ$), and low sliding angle. Owing to many applications of SHS (such as water-resistant surfaces, antifogging surfaces, anti-icing surfaces, anticorrosion surfaces, etc.), the artificial SHS could be prepared. This review article focuses on the deposition, behaviour and application of the SHS. It includes an introduction, fundamental principles of superhydrophobicity, main factors for SHS fabrications, deposition methods used to prepare the SHS, and factors affecting the electrochemical synthesis of electroconducting polymers. Moreover, the mechanism of the electrochemical synthesis of polymers, applications of SHS in different fields, and the stability of SHS have been presented. Finally, the challenges of SHS have been discussed.

Keywords: Superhydrophobic surfaces (SHS); Wetting behavior; low surface energy material; conducting polymer; Polyaniline; Polypyrrole

Contents	Page
1. Introduction	2
2. Fundamental Principles of Superhydrophobicity	4
3. Main factors for SHS fabrication	6
4. Deposition methods used to prepare the SHS	7
5. Factors affecting on the electrochemical synthesis of electro-conducting polymers	11
6. Mechanism of the electrochemical synthesis of polymers	13
7. Applications of SHS in different fields	15
8. The stability of SHS	17
9. Limitations in using SHS	17
10. Challenges of superhydrophobic surface	17
11. Conclusions	18
12. References	18

*Corresponding author e-mail: monahasnan1287@yahoo.com

Receive Date: 14 August 2020, Revise Date: 23 September 2020, Accept Date: 05 October 2020

DOI: 10.21608/EJCHEM.2020.39234.2803

©2021 National Information and Documentation Center (NIDOC)

List of abbreviations

Superhydrophobic surfaces	SHS
Photovoltaic	(PV)
Water Contact angle	WCA
Contact angle	CA
Contact angle hysteresis	CAH
Polystyrene	PS
Dimethylformamide	DMF
Tetraethoxysilane	TEOS
Isobutyltrimethoxysilane	IBTMS
Poly(vinylidene fluoride)	PVDF
Layer-by-layer	LBL
Poly (diallyl dimethyl ammonium)	PDDA
Poly (sodium 4-styrenesulfonate)	PSs
Glow discharge electrolysis	GDEP
Chemical vapor deposition plasma	CVD
physical vapor deposition	PVD
Carbon nanotubes	CNTs
Catalytic chemical vapor deposition	CCVD
Standard Calomel Electrode	SCE
Polyaniline	PANI
Polypyrrole	PPy
Indium-tin oxide glasses	ITO glasses
Cyclic Voltammetry	CV
Molecular weight	MW
Titanium isopropoxide	TTIP
Nano particles	NPs
Graphene Oxide	GO
Deionized water	DIW
Standard calomel electrode	SCE
Field emission-scanning electron microscope	FE-SEM
Nanometer	nm
Binding Energy	B.E

1. Introduction

Hydrophilicity and hydrophobicity are the most distinguishable definitions in surface science. In the Greek words, hydro means water, philicity means affinity, and phobicity means lack of affinity [1]. The surface would be hydrophilic if its static touch angle of water is $< 90^\circ$ and if $> 90^\circ$ is hydrophobic, as shown in Fig.1.

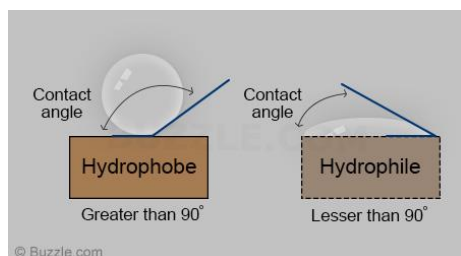


Fig. 1. Contact angle of hydrophilic and hydrophobic surface.

The contact angle of a liquid droplet is a suitable way of describing the wetting behaviour of the surface. It can be defined as the intercept of the droplet base line and the droplet tangent. The contact angle can be related to the surface energies of the three interfaces where air, liquid and solid meet as described by Young's equation [1]:

$$\cos\theta = \frac{\gamma_{SG} - \gamma_{SL}}{\gamma_{LG}} \dots\dots\dots (1)$$

Where θ is the contact angle, γ_{SG} , γ_{SL} , and γ_{LG} are the surface energies of the solid-gas, solid-liquid and liquid-gas interfaces, respectively as revealed from Fig.2.

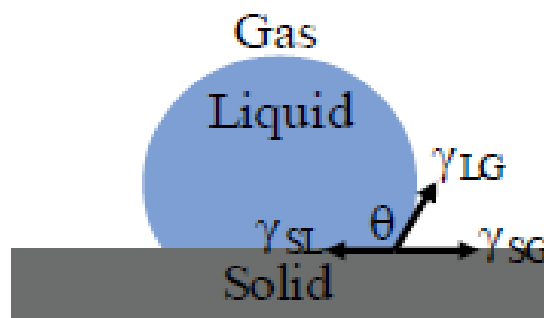


Fig. 2. The interfacial energies of droplet resting on solid surface [2].

The contact angle " θ " is a quantitative measure of the wetting of a solid by a liquid. It is the angle formed by a liquid at the three-phase boundary where a liquid, gas, and solid intersect. Theta optical tensiometer was used to measure the contact angle of the photovoltaic (PV) panel with and without the coating. Wetting behaviour of the solid surface can be divided into four different categories, depending on the value of the water contact angle (WCA). The two most traditional categories are the hydrophilic and hydrophobic, in which water contact angles in the range of $(10^\circ < \theta < 90^\circ)$ and $(90^\circ < \theta < 150^\circ)$ respectively [3]. The other two categories are superhydrophobic and superhydrophilic which describe the extremes of surface wetting behaviour, superhydrophobicity is characterized by WCA ($\theta \geq 150^\circ$), which describe the state of perfect non-wetting, unlike superhydrophilicity, described by WCAs ($\theta \leq 10^\circ$), in which at the first second of wetting the surface reach to the perfect wetting as shown in Fig. 3.

Superhydrophobicity is one of the research hotspots in surface science that has recently received significant attention both from fundamental and technological applications, due to the wide range of applications. Although superhydrophobicity has been studied since 1930, the interest and development in this phenomenon have grown intrinsically in the past few years due to recent admission of its potential applications in various areas [4]. Superhydrophobic

surfaces (SHS) show exceptionally high-water resistance. As water droplets fall on a SHS, they can quickly slide off the surface and dissolve dust particles along their sliding path. This property is known as self-cleaning that is favourable for outdoor optical devices such as solar cell panels or satellite dishes [3, 4]. Typical SHS discovered in nature have shown multi-scaled roughness consisting of nanometer-sized flakes on top of micrometer-sized protrusions. This form of morphology for superhydrophobic surfaces may be produced using pathways such as lithographic, template-based, plasma treatment, self-assembly and self-organization, chemical deposition, layer-by-layer (LBL) deposition, colloidal assembly, phase separation, and electrospinning. Most of these SHS are fabricated by complicated procedures or expensive facilities, which restricts their extensive applications. The development of large, long-term preserved SHS with simple and low-cost approaches remains a major challenge.

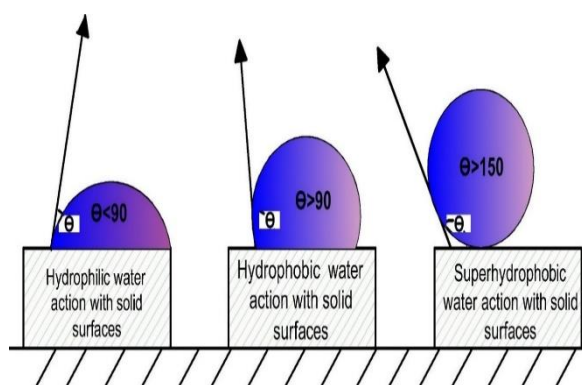


Fig. 3. Schematic diagram of water contact angle (WCA) dropped on solid surfaces.

Woodward et al. (2000) stated that, when surface energy is lowered, hydrophobicity is enhanced [5]. Chemical compositions determine the surface free energy which affects directly wettability. Nishino et al. (1999) reported that there are certain limitations are faced and superhydrophobic surfaces cannot be obtained only by lowering the surface energy [6]. For example, –CF₃– the finished surface was shown to have the lowest free energy and the best hydrophobic value, but the maximum contact angle on flat surfaces could only be 120°. Surface morphology plays an important part in the superhydrophobic material which affects the wettability of the surface. Wenzel et al. (1936) have shown that surface roughing can only improve its hydrophobicity due to an improvement in the solid-liquid interface, but also when air can be trapped on a rough surface between the surface and the liquid droplet [7]. Because air is a fully hydrophobic medium with a 180° contact angle, this air trapping should intensify the hydrophobic surface (Ogihara et al., 2013) [8]. So, the hierarchical micro- and

nanostructure of the surface are responsible for superhydrophobicity [3]. Neinhuis et al. (1997) reported the water contact angles of more than 200 plant species and investigated their surface morphologies as shown in Fig.4 [9].

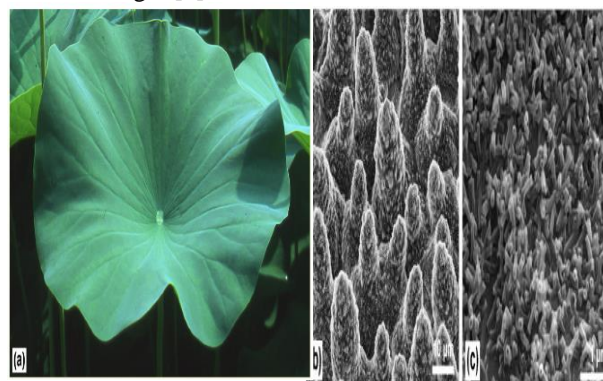


Fig. 4. (a) Lotus leaves (b) SEM image of the upper leaf side shows the hierarchical surface structure consisting of papillae, wax clusters and wax tubules. (c) Wax tubules on the upper leaf side [10].

Otten et al. (2004) revealed that there are two distinct types of water-repellent plant leaves: the first type is hair-covered leaves such as Lady's Mantle, and the second type is macroscopically smooth leaves such as Lotus. The droplets of waterfall absolutely off the leaves of both plants and their surfaces stay dry even after heavy rains [11].

Although several plants exhibited close touch angles (about 160°), the lotus leaves displayed greater stability and perfection than the water repellent. Such findings contributed to the principle of the "Lotus effect" and made the Lotus plant an archetype and an ideal model for superhydrophobicity. Some work has shown that the contact angle alone is not adequate to examine the effectiveness of superhydrophobic samples [3].

Lotus effect in plants

For a lotus leaf, the water contact angle found to be 162° (Fig. 5a) which represent the superhydrophobicity and the contact angle hysteresis (CAH) was about 2° which is very low value [12]. The superhydrophobicity and low CAH work on enhancing self-cleaning property for the lotus leaf.

Investigation of microstructure revealed that the lotus leaf was composed of micro scale papillae (Fig. 5b), and each single micro papilla consisted of many nano-sized nipples which form the hierarchical structure (Fig. 5c) [12]. By analyzing the surface chemistry of lotus leaf, it showed that the multiple micro /nanostructures were covered by a thin layer of wax, which reduced the surface energy of the lotus leaf. Moreover, the multiple micro/nanostructures crucially enhance the hydrophobicity of the surface, so the lotus leaf maintains the superhydrophobic state [12, 13].

The rice leaf is another popular example in nature display the “**lotus effect**”, in which water droplets bead up on leaf without wetting and spreading as shown in Fig. 5d [14]. However, the water droplet can easily roll off from the surface along the “a” direction, which parallels to the arrays of papillae (Fig. 5e). The water droplet adheres to the rice leaf when it is tilted in the “b” direction, which is perpendicular to the arrays of papillae (Fig. 5e). The microstructure of the rice leaf is similar to that of the lotus leaf: plenty of well-arranged microparticles are aligned on the surface, and each individual micro particle is composed of nanofibers. The length of these nanofibers reaches 1–2 μm , with a diameter of about 200 nm (Fig. 5f) [15].

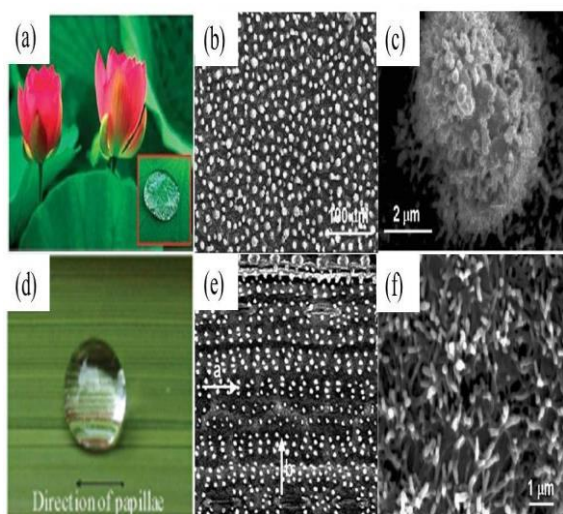


Fig. 5. The lotus effect in Plants [14].

Lotus effect in animals and insects

In addition to plant leaves, which have unique properties and behaviour, there are many animals and insects also exhibit their behaviour [12, 16-19]. By the investigation of the shark skin, it was found that the skin is covered by very small tooth-like scales named dermal denticles, polygonal with longitudinal grooves meaning that these grooves are aligned parallel to the flow direction of water. These grooves work on decreasing formation of vortices present on a smooth surface, leading to water moving over their surface [3].

Figure. 6a show the water strider which can walk quickly on water surfaces with its non-wetted legs. Gao et al. (2004) stated the investigation of the microstructure of strider legs; found that that their legs are covered with a mass of oriented micro-/nano-sized needle-shaped setae (Fig. 6b). These micro/nano-sized setae with fine nano grooves structures make air trapping, forming non-wetted air pockets that enhance the superhydrophobic state with a high WCA of $167.6^\circ \pm 4.4^\circ$ [12]. This enables water striders to survive on water surface.

The butterfly is another example in nature that displays superhydrophobicity. Its wings are superhydrophobic and self-cleaning which enables it to fly in the rain and maintains its cleanliness in the dirty environments. Figure. 6c, d show the SEM image of butterfly wings which revealed that superhydrophobicity is related to the hierarchical structures composed of nano-grooves/micro-anisotropic aligned sheets [16].

Cicada wings are also made of nanoscale pillars. The height of the nanopillars is in the range of 220–250 nm (Fig. 6e), the spacing between centres of nanopillars is about 110-140 nm [19]. The waxy layer on these uniform aligned nanopillars is the reason for the low surface energy, which increase the WCA (160°) and as a result enhance the superhydrophobicity of its wings.

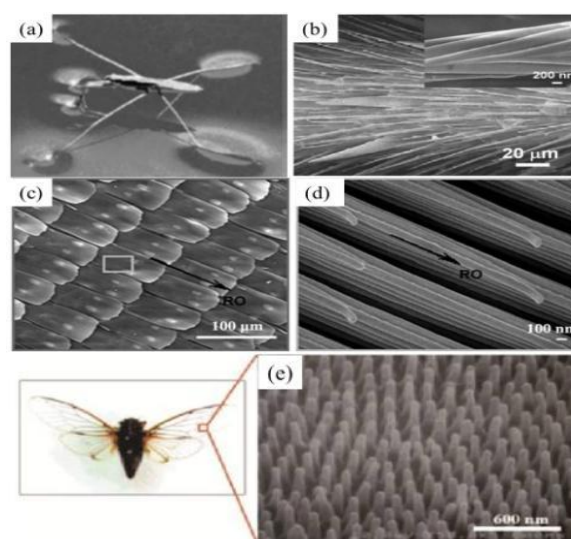


Fig. 6. The lotus effect in insects [14].

2. Fundamental Principles of Superhydrophobicity

2.1. Wetting behaviour on a solid surface

As mentioned before, the surface is said to be hydrophilic when the WCA is $< 90^\circ$, and hydrophobic when the WCA is $> 90^\circ$ as illustrated in Fig. 7 [20].

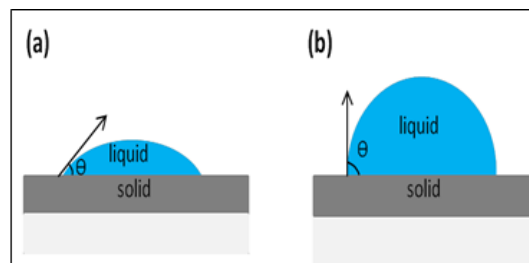


Fig. 7. Contact angle of a water drop on (a) hydrophilic, (b) hydrophobic surfaces [20].

For only chemically homogeneous and perfectly smooth solid surface, the contact angle of a drop can be calculated theoretically by the Young's equation [20], where:

$$\cos\theta = \frac{\gamma_{SG}-\gamma_{SL}}{\gamma_{LG}} \dots\dots\dots (2)$$

γ_{SG} : interfacial tension of the solid-gas interface,
 γ_{SL} : interfacial tension of the solid-liquid interface,
 γ_{LG} : interfacial tension of the liquid-gas interface.

The most predominant parameters to characterize the wetting behavior on any surface are the difference between the advancing contact angle (θ_{adv}), the receding contact angle (θ_{rec}) and contact angle hysteresis (CAH) as shown in Fig.8.

A superhydrophobic surface should has a high CA $>150^\circ$ and low CAH $<10^\circ$. The low CAH let water to roll-off easily along the surface [3].

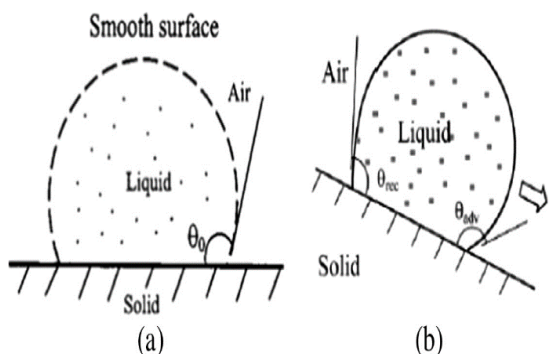


Fig. 8. Behaviour of a liquid drop on a (a) smooth solid surface, (b) tilted surface representing the advancing and receding CAs [21, 22].

The Young's equation is suitable only for flat surface, when the surface become rough, the Young's equation is not suitable [20]. The effect of roughness on the wetting of a surface was discussed by two different models, Wenzel in 1936 and then by Cassie and Baxter in 1944 [3].

2.1.1. Wenzel Model

Wenzel investigated the effect of surface roughness on wettability of the surface; found that the wettability is directly affected by the surface roughness of the wetted area. Water is in contact with the solid surface at all points, including cavities, which resulted in a greater actual contact area than what is observed (observed contact area calculated from the contact line of water droplet and substrate) as illustrated in Fig. 9 [23]. The contact angle in case of Wenzel model is given by the following equation,

$$\cos\theta_w = r \cos\theta \dots\dots\dots (3)$$

Where θ_w is the contact angle on a rough surface, θ is the Young's contact angle on a similar smooth surface, and r is the surface roughness factor, which is defined as the ratio between the actual and projected surface area. The roughness factor (r) >1 for a rough solid surface, and $= 1$ for a smooth one [24].

Wenzel's assumption was, for a hydrophobic surface $\theta_w > \theta > 90^\circ$ and for a hydrophilic surface $\theta_w < \theta < 90^\circ$. Since an extremely high roughness results in values of $\cos\theta$ greater than 1 or less than -1, this is not mathematically possible. In order to overcome this problem, Cassie and Baxter model developed the Cassie-Baxter model [25].

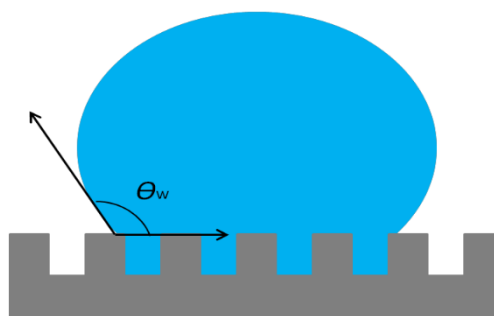


Fig. 9. Sketch of a water drop on a rough surface in case water penetrates the grooves (Wenzel model) [20].

2.1.2. Cassie and Baxter model (CB model)

The Cassie-Baxter model applicable for the composite or heterogeneous state, in which the grooves under the droplet are filled with vapour instead of liquid (liquid suspends on the grooves) as shown in Fig.10.

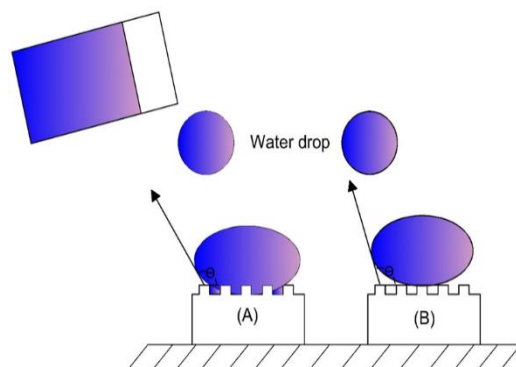


Fig. 10. Behaviour of a liquid drop on a rough surface, where, a) liquid penetrates into the spikes (Wenzel state), and b) liquid suspends on the spikes (Cassie-Baxter state).

Another model for heterogeneous surfaces supposed by Cassie and Baxter (1944) which composed of two fractions, one with a fractional area f_1 and contact angle θ_1 and the other with a fractional area f_2 and θ_2 , when ($f_1 + f_2=1$), The contact angle is given by equation.4[3]:

$$\cos\theta^{\circ} = f_1 \cos\theta_1 + f_2 \cos\theta_2 \dots\dots (4)$$

Where θ is the apparent contact angle, f_1 and f_2 are the surface fractions of the two phases, θ_1 and θ_2 are the contact angles of the two phases respectively.

For a rough surface containing only one type of grooves, using f as the solid fraction, the air fraction is $(1 - f)$. With $\theta = 180^{\circ}$ for air, the CA can be calculated by the following equation:

$$\cos\theta^{\circ} = f(1 + \cos\theta) - 1 \dots\dots (5)$$

Therefore, for the CB model, the apparent CA (θ°) is a unique function of solid fraction for a given surface with CA (θ). To obtain a superhydrophobic surface, the contribution of the solid part should be as small as possible or a solid surface with very high CA should be used. In fact, the CB model cannot predict accurately the wetting behaviour of a pre-designed surface. However, it is often used to compare it with a practical result in order to confirm the presence of the CB state. So, it can be concluded that, the two regimes of wetting behaviour are Wenzel state (completely penetration of liquid) and the Cassie–Baxter state (only suspension of the liquid) [24].

Comparing to Cassie model; the liquid droplet in Wenzel model show a higher sliding angle value [25]. Depending on the droplet conditions like impact, press and vibration, the solid/liquid contact mode will change from the Cassie to the Wenzel state [26, 27].

Zeng *et al.* recently exposed that the two states can get along with on a nano pillared surface. They display the mimicry proof of cohabitation of Wenzel/Cassie state for water droplets on a pillared hydrophobic surface. Depending on the initial location of the droplets, it was found that there were certain heights for the pillar after which the water droplets can be exist in the two states (Wenzel/Cassie) [28].

3. Main factors for SHS fabrication

To fabricate the superhydrophobic surface (SHS), two factors demonstrate the process which are; a) roughening the surface and b) low surface energy material [29-31].

Roughening hydrophobic materials that has low enough surface energy will be convert them to be superhydrophobic, careless to the exact value of the surface energy, therefore the roughness is the more critical property to achieve superhydrophobicity [32]. In order to fabricate SH, at least one of the following parameters must be included:

- 1-Roughening by incorporation of nanoparticles. i.e. (metal oxides)
- 2-Replication of natural surfaces (casting)
- 3-Addition of carbon nanotubes and surface modification by low surface energy materials [33-37].

3.1. Roughening a low surface energy material

3.1.1. Fluorocarbons

Fluorinated polymers are of particular interest due to their extremely low surface energies. Roughening these polymers leads to superhydrophobicity. Contact angle of poly (tetrafluoroethylene) (PTFE) (Teflon) surfaces is $115-120^{\circ}$ [4].

Shiu *et al.* (2004) used plasma etching for fluorinated polymers. The high energy oxygen species created by plasma can randomly etch fluorinated polymer materials and create surface roughness that required for increasing the water contact angle to be 170° [38, 39].

Additionally, Zhang *et al.* (2004) introduced a simple method to fabricate a superhydrophobic film by stretching a PTFE film. The formed film has a fibrous crystals structure containing some voids in the surface which play an important role in enhancing the superhydrophobicity. Moreover, Yabu and Shimomura (2005) success in the fabrication of porous SH membrane by casting a fluorinated polymer solution under humid environment [40, 41].

3.1.2. Organic materials

Organic materials demonstrated the fabrication of SHS, Lu *et al.* (2004) supposed a simple and inexpensive method to fabricate a highly porous SHS of polyethylene (PE) by controlling its crystallization behavior and the WCA was approximately 173° [42].

Jiang *et al.* (2004) displayed that, spraying and electrostatic spinning a polystyrene (PS) solution in dimethylformamide (DMF) leads to creation of SHS consisted of porous microparticles and nanofibers [43]. Lately, polyamide [44], polycarbonate [45] and alkylketene dimer [46] have been used for synthesis of SHS. Moreover, Yan *et al.* (2005) used electrochemical polymerization to fabricate a poly(alkylpyrrole) film, the structure of needle-like poly(alkylpyrrole) has been grown perpendicularly to the surface of the electrode was an environmentally stable superhydrophobicity [47].

3.1.3. Inorganic materials

For inorganic materials, which are naturally hydrophilic, the treatment of hydrophobic surface must be performed after the fabrication of surface structures [3]. Definite inorganic materials have been used made in fabrication of SH, for example, ZnO [48, 49], TiO₂ [50] have been used to produce superhydrophobic surfaces.

4. Deposition methods used to prepare the SHS

Several methods for the preparation of SHS were used, including sol-gel processing, electrospinning, spray coating, chemical and electrochemical depositions, layer-by-layer assembly, solution immersion, etching (laser, plasma, chemical), lithography, vapour deposition, colloidal assembling and polymerization [3, 12, 29]. Some of these methods will be discussed in the following section.

4.1. Sol-gel method

To get the SHS through the sol-gel method, the composition of the reaction and the sequence of the method must be pre-controlled. As a rule, a sol is prepared through hydrolysis and polycondensation of the corresponding oxide in the presence of solvent [51]. With a view to fabricate rough surface after the deposition of thin films, a minor ingredient is included during the process which can be easily removed by sublimation or dissolution in hot water, the removal of the minor ingredient creates the porous structures [4]. The most common precursor in sol-gel method was silicon alkoxides such as tetraethoxysilane (TEOS) referred to its advantages which are controlling size distribution and compatibility with other additives [52].

Roig et al. (2004) reported that Sol-gel processes can produce rough surfaces on different oxides such as silica, alumina, and Titania [53]. While, Shang et al. (2005) introduced a method to fabricate transparent SHS by modifying silica-based gel films with a fluorinated silane [54]. And, Xiu et al. (2008) fabricated SH isobutyl surface groups by blending isobutyltrimethoxysilane (IBTMOS) into silica layers and can reach to a contact angle of 165–170° [55]. It was found that the obtained surface was consisted of globules having diameter range (20–50 nm) surrounding a network of pores (submicron size), which confirms the hierarchical roughness in two scales which is the responsible on the high contact angle as shown in Fig.11.

Additionally, Barkhudarov et al. (2008) used organo-trimethoxysilanes as precursor to fabricate optically transparent SH films having WCA 155° and reaching 170° [56]. Lathe et al. (2009) prepared SH silica films on glass substrates using trimethylethoxysilane as a co-precursor. The product film was transparent, standard for harsh environment like humidity and high temperatures (up to 275 °C), having a WCA of 151° and a small sliding angle of 8° [57].

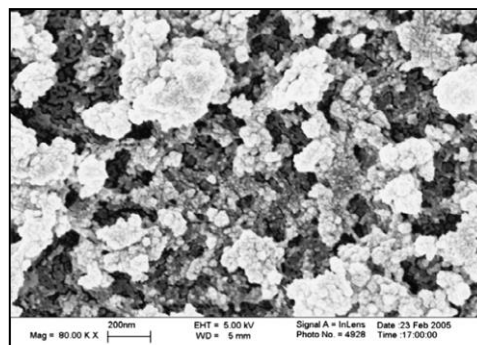


Fig. 11. SEM image of a silica film with a TMOS/IBTMOS ratio of 1:1 with high contact angle [3].

The advantages of the sol gel method in the preparation of SHS can be summarized as:

- Efficient method
- Low cost and low temperature
- High homogeneity of final products
- Produce rough surfaces on a variety of oxides
- Stability of the as-prepared coating due to the presence of covalent bonds between the coating and the substrate
- The formed coat is rough and robust [3, 52]

4.2. Electrospinning method

Electrospinning technique is a simple way in which different polymeric materials used to fabricate continuous fibers having diameters range from nanometer to submicron scale [3]. It is throwing process where an electrical bias is applied from the throwing nozzle and a grounded collector [51]. Adjusting the electro spinning process conditions, roughness with different scales can be controlled to fabricate the SHS as shown in Table.1 [58].

Table.1. Common Parameters of electrospinning technique [58]

Process Parameters	Material Properties	Equipment design	Ambient condition
Electrical field strength	Viscosity	Collector geometry	Temperature
Solution charge polarity	Conductivity	Needle design	Surrounding medium
Electrical signal type	Solvent volatility	-	Relative humidity
Flow rate	Polymer Type	-	-
Collector take up	Polymer MW	-	-
Tip to collector distance	Surface Tension	-	-

Electrospinning of fibers is an industrial applicable method to fabricate self-cleaning surface, but the ideally substrate for coating is on textile. Also, the fibers are lack of optical property and thermal stability [33]. Park *et al.* (2010) used the electrospinning method in the synthesis of mechanically durable, solvent-resistant, superhydrophobic nanofibrous mats, the precursor was poly (vinylidene fluoride) (PVDF) in the presence of tetraethyl orthosilicate (TEOS) and inorganic silane material [59].

Acatay *et al.* (2004) used electrospin method to deposit thin layer of fluorinated polymer onto a substrate made of an aluminium foil, by applying an electrical bias. The as-prepared electrospun film consisted of a continuous web of randomly aligned fibers [60].

Ma *et al.* (2005) stated that the fiber mats composed only of uniform fibers could be obtained by electrospinning a hydrophobic material like (poly (styrene-block-dimethylsiloxane) block copolymer) incorporated with homo polymer (PS) [61]. Moreover, Kang *et al.* (2007) synthesized PS fibers on silicon wafer using the electrospinning technique; the deposited film has superhydrophobic property and unique structure, which simulate the hierarchical structure of lotus leave [62].

Sanjay S. L. *et al.* (2012) used the electrospinning method to fabricate superhydrophobic Pullulan (PULL) from its natural source by the electrospinning of the fluorinated silane functionalized PULL. There was two weight percent of Pull membrane used (9 wt. % and 12 wt. %) the WCA recorded were only lower than 150° by electrospinning of pure PULL solutions. On the other hand, when the solutions of (9 wt. % and 12 wt. %) PULL coupled with fluorinated silane, the WCA reached to 155° and 151° respectively as shown in Fig. 12 [51].

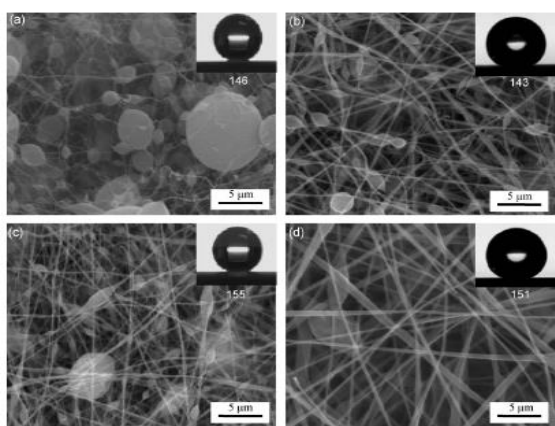


Fig.12. SEM images of prepared membrane where a) 9wt% Pull, b) 12wt% Pull, c) 9wt% Pull/PFOTES and d) 12wt% Pull/PFOTES [51].

4.3. Spray method

The spray method is thought to be effective technique to create SHS due to the large number of advantages which are: one-step method, cost-effective, economic, convenient for substrates with different shapes, time-saving, can be applied on the large industrial scale, and low temperature[57]. Great advantage of this method is the “repairing”, in case of mechanical damage of the surface; it can simply be repaired by partial spraying. Xu *et al.* (2011) synthesized superhydrophobic copper meshes via spraying method using an emulsion of silver nitrate and n-octadecanethiol in ethanol onto the copper mesh using nitrogen gas throw spray gun. The reason for using alkanethiols is that they contain long-chain alkyl groups that have low surface free energy[63].

Super hydrophobic paper was fabricated by Ogihara *et al.* (2013), fabricated using mixtures of ethanol and nanoparticles. The mixture was manually sprayed over the paper from a distance 20 cm with a vaporizer. Reaching to the most dominant factors in the fabrication of SHS i.e. (the roughness and surface energy) can be achieved by adjusting the spray conditions like the type and size of the used nanoparticles [8].

4.4. Layer-by-layer method

Layer-by-layer (LBL) deposition is mainly depending on the electrostatic charge interactions and hydrogen bonding between either polyanion and polycation or alternatively charged polyelectrolytes or nanoparticles to form different layers [4, 51]. The first experiment of a superhydrophobic coating fabrication using the LBL technique was reported by Zaho *et al.* (2005). They assembled a polyelectrolyte multilayer containing SiO_2 nanoparticles through and then heated the multilayer film to 650°C to create a surface having the superhydrophobic property [64].

Zhai *et al.* (2004) used LBL method to prepare a polyelectrolyte multilayer surface and then re-coated with silica nanoparticles to simulate the hierarchical structure that exist on the surface of lotus leaf. Superhydrophobicity was achieved after fluorination of the surface using a fluoroalkyl silane [65].

Amigoni *et al.* (2009) fabricated hybrid surfaces (organic/inorganic) by using different layers alternatively of epoxy-functionalized smaller silica NPs and amino-functionalized silica NPs. It was found that the hydrophobicity increases linearly with the number of layers. For alternation of nine layers, the obtained water contact angle was approximately 150°C [66].

Isimjan *et al.* (2012) constructed titanium thin films on steel substrates via LBL deposition process. Firstly, the precursor Poly (diallyl dimethyl ammonium) (PDDA)/Poly (sodium 4-styrenesulfonate) (PSS) was deposited on the surface of steel by three cycles of alternate immersion of the substrate in PDDA

and PSS aqueous solutions. Then, the substrate was alternatively dipped in TiO_2 P25 aqueous solution and PSS [67]. This stage was repeated many times in order to obtain multilayer films of $(\text{TiO}_2/\text{PSS})^*n$, where n refers to the number of deposition cycles. The obtained coatings on steel substrate achieved the hydrophobicity through the contact angle greater than 165° and strong repulsive force to water droplets as illustrated in Fig.13. The advantage of this technique is that:

- Simple and economic to permit controlling the thickness of the resulting layer [51].
- The linear growth of films with respect to the number of multiple layers, make this method success in controlling the film thickness [3].
- Also, the film thickness and roughness can easily be controlled by controlling number of deposition cycles and particle size [4].

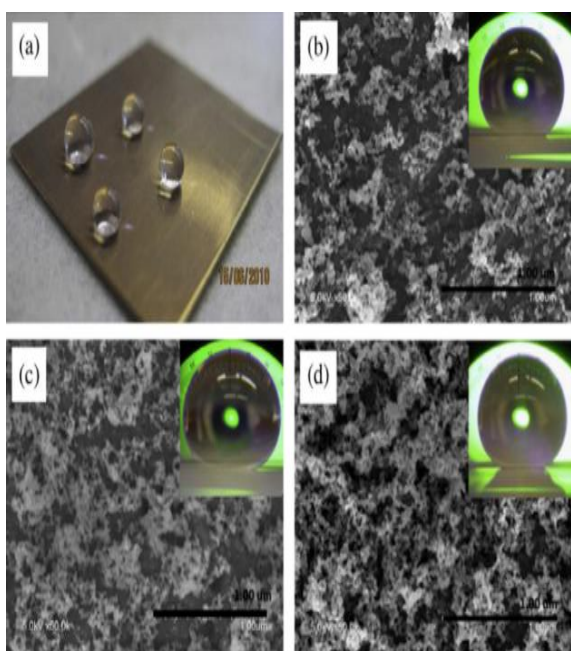


Fig. 13. SEM images of different layers of TiO_2 nanoparticles in steel surface: (a) Water droplets on the treated steel surface, (b) One layer $(\text{TiO}_2)^*1$, (c) TiO_2 two layers $(\text{TiO}_2)^*2$, and (d) TiO_2 three layers $(\text{TiO}_2)^*3$ Images reprinted from Ref. [67], with permission from Elsevier, Copyright 2012.

4.5. Solution Immersion Method

This technique has some advantages like time-saving and unless for the expensive precursors, easy to operate and no special equipment is required. Solution-immersion method for the fabrication of superhydrophobic surfaces on copper substrates was reported by Kong et al (2008). Figure 14 show the thin layer of $\text{Cu}_2(\text{OH})_3\text{NO}_3$ crystal that prepared on the surface of the copper foil by consecutive immersing in an aqueous solution of sodium hydroxide and cupric nitrate. Further treatment was made on the layer using

1H, 1H, 2H, 2H-per- fluoro decyl tri ethoxysilane (FAS-17) to obtain the superhydrophobic surface [68].

Li et al. (2008) used a commercially available, waterproof source like potassium methyl silicate (PMS) for fabricating superhydrophobic surfaces on cellulose substrate through a solution-immersion method as illustrated in Fig.15[69].

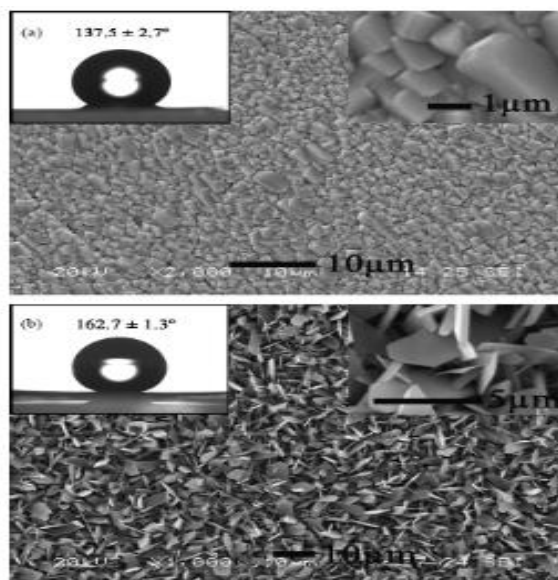


Fig. 14. SEM images of (a) CuO micro-crystal and (b) thin layer of $\text{Cu}_2(\text{OH})_3\text{NO}_3$ crystal. Images reprinted from Ref. [68], with permission from Elsevier, Copyright 2008.

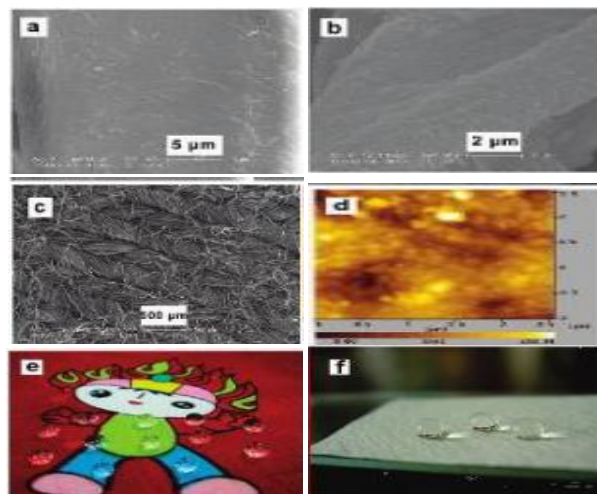


Fig.15. FE-SEM images of (a) the native cotton fiber, (b) the modified cotton fiber, and (c) the modified cotton fabric at low-magnification. (d) A three-dimensional AFM image of the modified fiber surface, (e) an image of water droplets on the surface of the modified colored cotton fabric, and (f) an image of water droplets on the surface of the modified filter paper. Images reprinted from Ref. [69], with permission from American Chemical Society, Copyright 2008.

4.6. Etching Technique

Etching is a simple and easy technique to fabricate SHS coating with rough surface. Dong et al. (2011) reported that there are different etching techniques like chemical, plasma and laser etching, have been recently used [70]. It was found that the chemical etching was a simple method to get rough surface on polycrystalline metal surfaces [71-73]. SHS fabricated on aluminium alloy grade AA2024 using hydrochloric acid as chemical etching solution, Li et al. (2012). It has been found that the chemical etching time play an important role in fabrication of SHS and rough surface. $WCA > 150^\circ$ was recorded at an etching time of more than 3 min [74].

Organic polymer like polypropylene and PTFE, and glass surfaces can be etched and roughened using plasma etching [75, 76]. SHS has been fabricated on zinc substrate using glow discharge electrolysis plasma (GDEP) reactor for etching, Gao et al. (2012) [77].

Another way for etching was laser etching which can be used for silicon surfaces, micrometer scale topographic structures such as grooves can be created with controlled width and depth with a high-power pulsed laser beam. After the roughening process, these surfaces can be treated with alkylsilane or fluorinated silane molecules to produce superhydrophobic properties [78].

4.7. Chemical and physical vapour deposition

Chemical vapor deposition (CVD) or physical vapor deposition (PVD) has been widely used in the modification of surface chemistry as well as the synthesis of nanostructured surfaces which make dramatically change in surface roughness that play an important role in hydrophobicity [79-81].

CVD technique involves the deposition of gaseous reactants onto a substrate forming a nonvolatile solid film. For mentioning the advantages of this technique, it is an efficient and preferred process to build and construct the micro-/nanoparticles, in order to simulate the hierarchical structure that exist in lotus leaf which is responsible for the hydrophobicity [53]. Hsieh et al. (2008) prepared a superhydrophobic carbon fabric with the scales (micro/nano scaled) two-row roughness by decorating carbon nanotubes (CNTs) onto micro sized carbon fibers, using a catalytic chemical vapour deposition (CCVD) and then followed by fluorination of the surface [82].

4.8. Chemical and Electrochemical Deposition Techniques

Chemical and electrochemical deposition techniques have been widely used to fabricate SHS [2]. These techniques are independent of the shape and size of the substrate. In addition to electrochemical deposition, other electrochemical methods have been

used to fabricate SHS, such as electrochemical polymerization, non-electric chemical plating, anodically oxidized methods and galvanic cell reactions [83].

Electrochemical polymerization has specific advantages due to polymerization rate easily controlled by varying oxidation potential, media of polymerization can be reused, doping process exist simultaneously, and a better control film thickness and morphology, and cleaner polymers can be produced.

The electrochemical methods can be divided into three main categories: galvanostatic, potentiodynamic (cyclic Voltammetry), potentiostatic, step current method, and step potential methods. All of these methods are, a three-electrode system consists of working electrode on which the polymer is deposited, a counter electrode (platinum rode) and a reference electrode (the most common on is a saturated calomel electrode (SCE). The most common working electrodes are platinum, conducting glass (glass covered by indium-doped tin oxide (ITO) electrode), stainless steel, graphite, Au, Fe, Cu, etc. [84].

4.8.1. PANI films prepared by electrochemical method

PANI films prepared by electrochemical method have an excellent photoelectric property, which can be applied in the area of the fabrication of luminescent material [85]. With respond to nanostructure, electrochemical performances of PANI materials can be enhanced which is primary due to their unique characteristics of conducting pathways and surface interactions. Nowadays, nanowires tubes [86], nanoparticles [87], nanofibers [88], nanorods [89], nanowires [90] of PANI have been widely studied and the researches regarding new materials which possess the advantages of both small-scale systems and organic conductors are undergoing.

The most two effective parameters that determine the chemical structure of PANI are the doping level and the redox state. PANI has three well defined oxidation states. Firstly, the half-oxidized state (emeraldine). Secondly, the fully oxidized state (pernigraniline). Lately, the fully reduced state (leucoemeraldine), with an infinite number of possible oxidation states existing in between.

Figure 16 shows the general chemical structure of PANI, where the polymer backbone composed of two different types of repeating units; the oxidized and the reduced unit. The degree of oxidation is characterized by the mutable (x) whose value is ranging from (0 to 1), and it represents the fraction of the two repeating units. Therefore, pernigraniline, emeraldine, leucoemeraldine refer to the chemical formula where $x = 0, 0.5$ and 1 respectively [91].

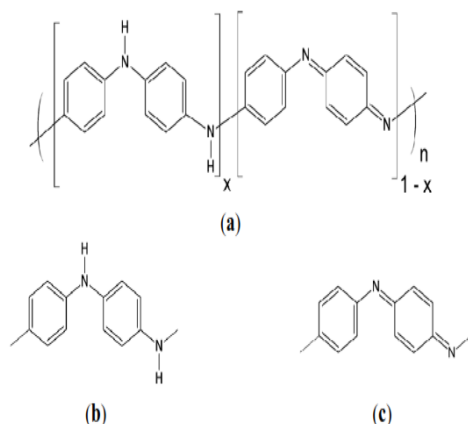


Fig. 16. Chemical structure of polyaniline and its repeating units, (a) A general chemical structure of polyaniline, (b) Reduced repeating unit, and (c) oxidized repeating unit[91].

The oxidized repeating unit contains only imine nitrogen atoms with the absence of any hydrogen bonds which can be easily protonated in an acidic medium, where these nitrogen atoms can be attacked by protons to form radical cations [92, 93]. On the other hand, the reduced repeating unit contains only the amine nitrogen atoms. The degree of protonation mainly depends on pH of the aqueous solution in which the polymer is immersed and the oxidation state of PANI. It was believed that protonation occurred on the imine nitrogen atoms, but, experimental results revealed that some amine nitrogen atoms can also be protonated to form NH_2^+ groups even if all the imines are not protonated [94-97]. The unprotonated form of PANI is known as a base while the protonated form is known as a salt. Figure 17 shows the three different redox states of polyaniline in their base forms and the corresponding salts.

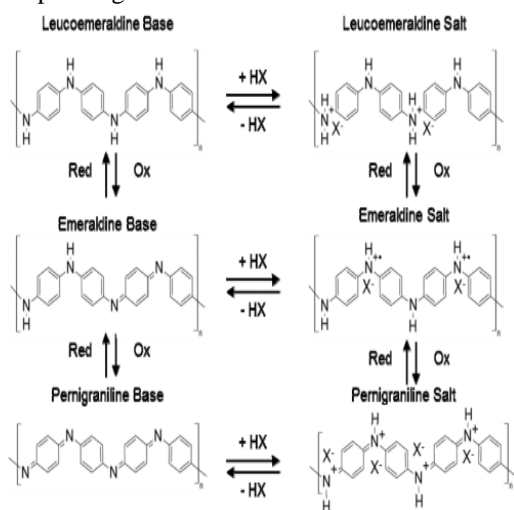


Fig.17. Redox states and the doped form of polyaniline [91].

4.8.2. Polypyrrole films prepared by electrochemical method

Polypyrrole (PPY) film was fabricated having conductivity of 8 S cm^{-1} using electrolysis of pyrrole solution in acidic solution of sulfuric acid; it was found that the deposited layer of the polymer on the surface of working electrode was in the powder form [98]. While Diaz et al. obtained flexible form of PPy the polymer with conductivity of 100 S cm^{-1} [99, 100]. The working electrode for electrochemical synthesis of conducting polymers is usually made of corrosion-resistant materials that are standing for high oxidation potential, namely like (Ir, Rh, Pt, Pd, Au) [101-103]. Also conducting glasses were used as a working electrode like SnO_2 , In_2O_3 [104, 105].

PPy prepared by oxidation of the monomer with chemical oxidants has a form of black powder. The chemical oxidants that were used like: aqueous or anhydrous FeCl_3 , other salts of iron (III) and copper (II). Also, organic electron acceptor and halogens were used as an oxidant. S. P. Armes (1987) reported that the yield of PPy can be reached to 100% by using optimal ratio of Fe (III) / monomer ~ 2.4 . Lower temperatures (0 to 5°C) and shorter times of process resulted in enhanced conductivity of PPy [106]. S. Machida, et al. (1989) succeed preparation of PPy by monomer oxidation with FeCl_3 in different solvents (acetone, water, acetonitrile (AN), alcohols, benzene, tetrahydrofuran, chloroform, dimethylformamide), and found that the highest conductivity (190 S cm^{-1}) for PPy was achieved using methanol [107].

5. Factors affecting on the electrochemical synthesis of electroconducting polymers

Taking in our minds the similarity of the proposed mechanisms of electrochemical and chemical synthesis of electroconducting polymers, it is reasonable to expect that the factors affecting the chemical and electrochemical synthesis of electroconducting polymers are also similar [108]. In addition to the composition of reaction solution, *i.e.*, electrolyte, and temperature, the electrochemical synthesis is strongly affected by the influence of the electrode material and selected electrochemical technique [109-112].

Zhang et al. (2004) reported that, the possibilities of oxidative polymerization are affected by the ability of the monomer to be soluble in the aqueous acidic solution and by their ability to create salts in an acidic environment [113]. The process of aniline oxidation is an exothermic reaction. The released heat can be used to monitor the course of the reaction. The success of aniline polymerization with oxidation agents is completed only in an acidic media in which aniline exists in the cation form [114].

Factors affecting on the electrochemical synthesis of electroconducting polymers can be summarized as:

5.1. Electrolyte composition

Most of the electrochemical syntheses of electroconducting polymers are performed in aqueous electrolytes depending on the facts of environmental concerns, the price, easy of handling and the ability of using various dopants [115]. There is limited number of studies interested in the electrochemical polymerization in non-aqueous solvents. Miras *et al.* (1991) informed that acetonitrile is the most common solvent used in the electrochemical polymerization [116]. Dichloromethane, nitrobenzene, propylene carbonate and recently the application of ionic liquids was also considered [117-121].

Heinze *et al.*, (2010); Innis *et al.* (2004); Li *et al.* (2005) worked on the electrochemical polymerization of aniline in different ionic liquids. IR and NMR spectroscopy showed that the ionic liquid (1-ethyl-3-methylimidazolium ethyl sulfate) was incorporated in polyaniline during electrochemical polymerization [122-124]. To reach the complete solubility of the monomer, the solvent should be stable at potentials and pure as possible. For example, the presence of dissolved oxygen may cause a problem due to reaction with radical intermediates and it can be also reduced at counter electrode and forms hydroxide. There is a great problem that cannot be neglected which is the interaction of the monomers, solvent and electrode materials, where it has an impact on monomer adsorption onto electrode [117].

5.2. Electrode material

The nature of the electrode affects the ability of the monomer oxidation; on the other hand, deposition of the polymer on the electrode is dependent on the surface energy of the electrode and its hydrophilicity/hydrophobicity [115]. Inert electrodes such as: indium-tin-oxide (ITO) glasses, platinum, gold, graphite, glassy carbon; are very suitable electrodes for the electrochemical polymerization of aniline. But the major limitations of the usage of other materials released from the fact that relatively high electrode potential is required for oxidation of aniline to complete the electropolymerization process. On this necessary high potential for the oxidation of aniline, either the active metals like (iron, steel, copper...) will be dissolved or form a low or nonconductive passive layer in case of (aluminum and its alloys). This problem should be considered when electrochemical synthesis is applied for corrosion protection application [125-129].

In case of steel and aluminum, the most common electrolyte used to electrochemical synthesis of polyaniline is oxalic acid [130-133]. Using oxalic acid allows the growth of passive layer that consist of iron oxalate, on which the process of aniline polymerization occur. Camalet *et al.* (1998) reported that p-toluene sulfonic acid can be used in polymerization of aniline after the formation of passive

layer. While in case of oxalic acid, the passive film was consisted mainly of iron oxide [134].

Electrochemical polymerization process of aniline on zinc and mild steel from an aqueous solution consisted of two-steps; the first step is the electrodeposition of a thin film of polypyrrole. It acts as a pretreatment step of the surface and completely modification for its electrochemical response to the traditional acidic solutions used for the second step electropolymerization of aniline. The films show stable electroactivity in acidic electrolytes, similar to that of PANI deposited on platinum, which indicates that the underlying oxidizable metal is fully protected [131].

5.3. Electrochemical techniques

According to the electrochemical polymerization techniques, the properties of the deposited film of electroconducting polymers can be changed. Electrochemical techniques can be categorized into three types: potentiostatic, potentiodynamic, galvanostatic and electrospinning techniques [117].

a) Potentiostatic Growth

In this method, a constant value of positive potential (for oxidative polymerization) is applied potential. It is necessary to choose the potential high enough for polymerization to occur. On the other hand, potential has to be low enough to avoid undesired secondary reactions and over oxidation of the polymer [135, 136]. In this technique the obtained polymer is in doped state. Modified pulse method can also be used. In pulse potentiostatic technique alternating anodic and cathodic pulses of constant potential is applied. During the cathodic pulse, dedoping of the polymer occurs, while at the anodic pulse, the electrochemical polymerization and deposition of the polymer are occurred [136].

b) Potentiodynamic Growth

Potentiodynamic method involves scanning the potential of the working electrode directly from the start to the final value in both forward and backward (reverse) directions (Cyclic Voltammetry technique) repeatedly until the desired amount of polymer has been deposited [137, 138]. In this technique, sweeping the voltage is very useful for understanding and investigation the redox mechanism of the monomer [139]. It was shown that nanostructured electroconducting polymers can be obtained by this method. Using this technique, the deposited PANI film changes between its non-conducting (dedoped) and conducting (doped) form [122]. It has been reported that by applying the CV method, more uniform film of PANI deposited compared to that formed at constant potential and promotes better adhesion to the electrode surface.

c) Galvanostatic growth

Galvanostatic technique refers to formation of electroconducting polymer via keeping the flowing constant current value. At the end of polymerization process, the obtained film is in doped (conductive) form [122]. The advantage of this technique is controlling the thickness of polymer film by adjusting the duration of the polymerization process. Implementation of galvanostatic technique requires suitable selection of the current density used in the polymerization process. The resistance will increase due to the growth of the polymer film at the surface of working electrode; this action resulted in increase in the potential. Increase of the potential promotes side reactions, so reducing the polymerization efficiency [135].

d) Electrospinning technique

Electrospinning method include fiber production which uses electric force to draw charged threads of polymer solutions or polymer melts up to fiber diameters in the order of some hundred nanometers. The electrospinning technique has been investigated by Huang et al. as a new method of PANI synthesis [140, 141]. Wang et al. used an in-situ electrochemical growth method to produce PANI and PPy nanowires within a microfluidic device [142].

5.4. Doping anions

Usually, electrochemical polymerization of aniline is carried out in strong acidic aqueous electrolytes. Doping anions originate from the acid and represent its conjugated base. The dopant anions are inserted during electrochemical polymerization and therefore their concentrations affect directly on the morphology, conductivity, and electrochemical activity of formed PANI and also on the polymerization process itself [143-146]. It was proved that PANI was obtained in the presence of "large dopant anions", represented in sulfuric acid, hydrochloride acid, sulfosalicylic acid, nitric acid and p-toluensulfonic acid. The presence of these anions enhances the formation of more swollen and open structured film. The presence of "small ions" such as ClO_4^- or BF_4^- resulted in formation of a more compact structure [147, 148].

6. Mechanism of the electrochemical synthesis of polymers

6.1. Mechanism of the electrochemical polymerization of PANI

The process of electrochemical polymerization of PANI is always carried out in strong acidic solutions ($\text{pH} < 2$). Increase in pH would lead to formation of short conjugation oligomers materials having different materials [117, 149]. The steps of electrochemical polymerization of PANI can be summarized in the following steps:

1-The first step of the polymerization process was the oxidation of monomer in which occurs the

formation of radical cation as shown in Fig.18. It was considered to be the rate determining step [150, 151].

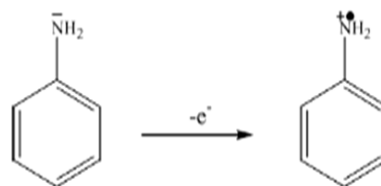


Fig.18. Aniline cation radicle[152].

The abundance of aniline radical cation was confirmed by adding some substances like (benzoquinone, hydroquinone, resorcinol, etc.) having the ability of retarding the reaction, which indicating the proceeding mechanism was a radical mechanism [152]. According to Inzelt, 2008, the oxidation of aniline monomer is an irreversible reaction, occurring at higher positive potential (0.9 V vs. standard calomel electrode) than PANI redox potential [153]. The aniline radical cation has three resonance forms, represented in Fig.19. Across these three resonance forms, the most reactive one is form (2) due to absence of steric hindrance and its important substituent inductive role. Finally, the oxidation of the monomer leads to formation of soluble oligomers [154].

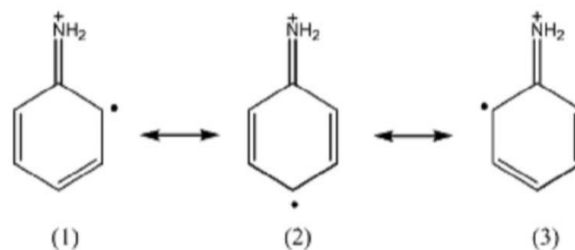


Fig.19. Different Resonance forms of aniline radical cation [152].

2- The second step, deposition of oligomers on the anode surface occurs through nucleation and growth process.

3- The third step as illustrated in Fig.20, occur coupling of radical cations formed from oligomers and aniline radical cation leading to chain propagation (Dimerization).

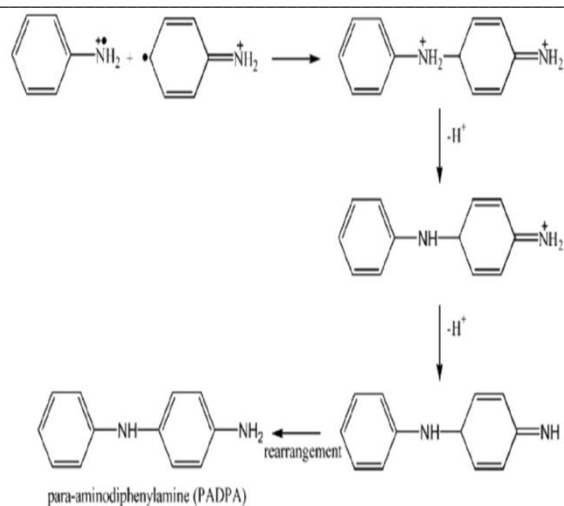


Fig. 20. Schematic diagram of dimerization [152].

Finally, the formed radical cation can react either with the radical cation monomer or with the radical cation dimer to form a trimer or a tetramer and finally polymer is formed, as shown in Fig.21.

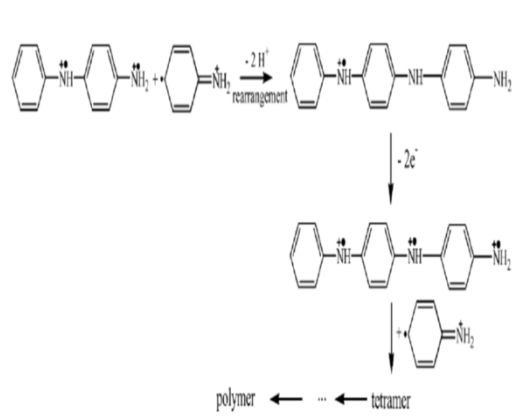


Fig. 21. Schematic diagram of polymer formation [152].

It was alleged that the process of electrochemical synthesis of polyaniline is an autocatalytic process. It can be declared as; the formation of the polymer on already deposited polymer proceeds faster than on the bare electrode meaning the higher rate of polymerization. Well defined confirmation for the evidence of autocatalytic process using cyclic voltammetry technique. It was found that that current increased over time for potentials higher than 0.8 V (vs. saturated Calomel Electrode) and that anodic peak potentials decreased. The increased intensity of the anodic peak currents was connected to increased polymerization rate, while decrease of the anodic peak potentials was assigned to facilitated electrochemical polymerization [155].

6.2. The mechanism of electrochemical synthesis of polypyrrole

Unlike polymerization of aniline, polymerization of pyrrole can be successfully achieved in neutral aqueous environment and also different organic solvents. Among the proposed mechanisms of electrochemical polymerization of polypyrrole, only two have gained the greatest interest. One of those is the oxidative coupling of monomer molecules, and the other is the reduction.

First proposed mechanism

1-The first step of the reaction refers to the oxidation of monomer molecules yielding radical cation as shown in Fig. 22 [151]. Unpaired electron and positive charge are delocalized at α position, meaning that this position is the most reactive one. Therefore, this position is ready for the radical coupling.

Pyrrole oxidation

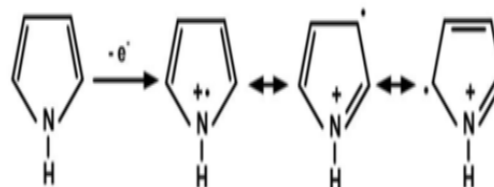


Fig. 22. Formation of pyrrole radical cation [115].

2-The second step is the coupling of two radical cations, leads to formation of positively charged dimer which is the rate determining step of reaction. Referring to the strong conjugation, the formed dimer is oxidized easier than radical cation under the given reaction conditions leading to the further step as shown in Fig. 23 [156].

Formation of dimer

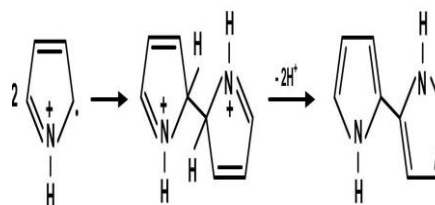


Fig. 23. Coupling step (Dimerization of cation radicle)[115].

3-The third step is the oxidation of the dimer that formed in the previous step therefore occurring at the lower potential, leading to formation of new radical cation as shown in Fig.24.

Oxidation, coupling and rearomatization

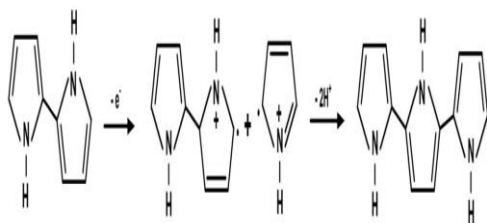


Fig. 24. Oxidation of the dimer [115].

4-The final step is the chain propagation, leading to polymer formation as represented in Fig. 25.

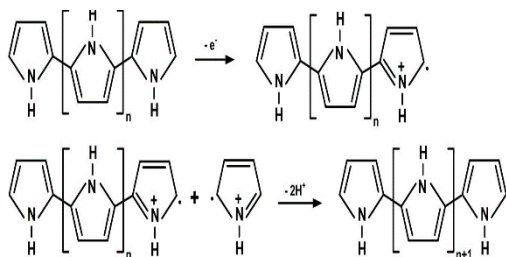


Fig. 25. Chain propagation[115].

Second proposed mechanism

1- The first step is the formation of a radical cation on the anode.

2- The second step is the loss of a proton and attack of the radical on a neutral monomer.

Finally, after the reoxidation of the proton loss and dimeric radical, the dimeric molecule also oxidized, which results in chain growth[157].

7. Applications of SHS in different fields

By reporting the different ways of fabricating SHS, it is now easy and simple to choose the best method through several superhydrophobic treatments which is suitable for target substrate materials. For example, high transparency is an important property for many optical applications. While the surface roughness increases the hydrophobicity, the scattering of light by rough surfaces decreases the transparency. Since the visible light wavelength is 400–750 nm, the surface roughness for transparent superhydrophobic films should be less than 100 nm. Another issue is the

degradation of superhydrophobicity due to accumulation of stains over long times of outdoor exposure. Implication of TiO_2 can relieve this problem through photocatalytic decomposition of deposits. This is another active research area in this field. In some applications, surfaces responsive to external stimulations are highly attractive [4].

Bhushan and Jung (2011) illustrated that, reason for development of materials with SH properties was for using in practical applications. SHS have gained great interest in the past two decades due to their unique self-cleaning property, water repellency. These properties are favorable for many industrial and biological applications such as antibiofouling, anti-corrosion, solar panels, self-cleaning windows, paints for boats, metal refining, the separation of water and oil, and in the textile industry such as in the manufacture of water-proof, fire-retardant clothes and glass building [21].

7.1. Anti-biofouling applications

Biofouling is the accumulation of microorganisms, plants, algae, or small animals on wetted surfaces that have a mechanical function, that cause decreasing in structural functional efficiency.

Townsin (2003); Gudipati et al. (2005) mentioned that biofouling of underwater structures and ships' hulls increases the cost for both maintenance and operation [158, 159]. The huge cost can be reduced through underwater superhydrophobicity by forming a hydrophobic rough surface that supports an air film between itself and the water (Trapping for the air). The reduction of the wetted area works on decreasing the probability of incorporation of biological organisms into solid surface.

Zhang et al. (2005) investigated the anti-biofouling properties of superhydrophobic coatings compared to normal substrates, which fouled within a day, and found that almost no micro-organisms attached to the SHS in the first week after immersion [160].

7.2. Self-cleaning

Self-cleaning surfaces are mainly based on high water contact angles ($\geq 150^\circ$). A drop of water on the surface is almost spherical and readily rolls off taking the dirt away with it. For window glasses applications, the high-water contact angle (above 150°C) and the low contact angle hysteresis of SHS are very effective factors that characterize them with low adhesion and self-cleaning properties. In a natural environment, surfaces gradually become contaminated and cleaning them requires great effort additionally, surfactants that used in cleaning have a negative effect on the environment.

Nimitrakoolchai et al. (2008) investigated the self-cleaning properties of a superhydrophobic film by applying red powder and dust onto the film. The way for roughening the surface was the deposition of a

polyelectrolyte film on a glass substrate, followed by etching in HCl solution and then deposition of SiO₂ nanoparticles onto the etched film. It was found that much of the red powder was still exist on the uncoated glass surface even after cleaning with water droplets as compared to the SHS, which was cleaner [161].

Self-cleaning property for the SHS plays also an important role in textile industry. Xue *et al.*, 2010, have been synthesized self-cleaning textile like skirts, trousers, shirts and blouses, which are stain-proof [162]. On the other hand, the self-cleaning property is also used in optical applications, such as lenses, a solar panels and mirrors that need to be stay clean. An advantage of superhydrophobic textiles is that the fibrous structure can be maintained while keeping the fabrics breathable, which is preferable to traditional waterproof textiles treated with rubbers, plastics, sealing agents, or a conventional wet-chemical finish using fluorocarbons. Additional benefits of the superhydrophobic effect on textiles could include a plastron layer [22].

STO Corp. (USA), a manufacturer of high-quality building materials, has been marketing an exterior paint since 1999 under the trade name Lotusan. The product was a highly water-repellent surface similar to that of the lotus leaf. Its microstructure has been modelled on the lotus leaf to minimize the contact area for water and dirt. The surface additionally offered high resistance to the growth of mold, mildew algae.

The Swiss firm Schoeller Textil AG developed a technology called "Nano-sphere". In this technology, nano silica particles or a polymer were attached on the clothing fibers, and these particles provide lotus like bumpy roughness, making textiles superhydrophobic and self-cleaning.

With Mincor TX TT, BASF has made it possible to fabricate textiles with a self-cleaning effect based on nanostructured surfaces. This finishing material has the same self-cleaning effect as the lotus leaf. Particles having a diameter below 100 nm doped in a carrier matrix on the treated textile mimic the very small papillae found on the surface of the plant leaves and repel water droplets. Dirt particles were carried away by the water droplets and were washed without the need for detergents or scrubbing.

Moreover, dust accumulation on solar collectors disrupts the intended function of the solar panel at that first surface/light interface, which can significantly reduce the power output and efficiency or can completely terminate system operation. Dust is not a major concern in areas that have low-soiling conditions and/or periodic precipitation that cleans the surfaces naturally. Extensive research on the accumulation of sand and dust on the surface of photovoltaic (PV) modules have been carried out in the past 15 years [163, 164].

Both field studies and laboratory experiments have shown that dust has a negative impact on the performance of PV. Dust particles block incident photons from reaching the PV cells and consequently reduce the output electrical power from the module. This is a particular problem for dry regions such as the Middle East and North Africa where wind-driven sand and dust particles are a characteristic of the local environment. These regions are favorable locations for PV installations as a result of high average irradiance levels and the availability of land. The study by Salim *et al.* into long-term dust accumulation on a solar-village PV system near Riyadh (Saudi Arabia) indicated a 32% reduction, after 8 months, in performance of the solar array due to dust accumulation [165]. Elminir *et al.* conducted one of the most comprehensive and revealing studies involving dust effects on solar collectors. Transparent covers of solar collectors were evaluated in Cairo, Egypt, examining the effects of tilt angle, orientation of exposure, climate, deposition density, and mineralogy of the dust. The research was conducted at the National Institute of Astronomy and Geophysics, within an industrial area in which several cement factories were co-located [166].

El-Shobokshy and Hussein [167] are credited as pioneers on a comprehensive study into the impact of dust on the performance of PV cells. The study included investigations into the physical properties of the dust accumulation and deposition density on their impact on parameters degrading PV efficiency. The experiment was entirely simulated with artificial dust (including limestone, cement and carbon particulates). The study revealed the impact of cement particles to be the most significant, with a 73 g/m² deposition of cement dust resulting in an 80% drop in PV short-circuit voltage.

Said [168] studied the effects of several months of dust accumulation in maritime-desert-zone type of environments on solar collectors which included a double-glazed flat-plate collector, an evacuate-tube collector with cylindrical reflectors and a PV panel. A 7% efficiency degradation rate of per month was found for PV. Monto. M, *et al.* have provided a compelling "guide" to soiling conditions and mitigation for various regions of the world because of substantial variation in the weather, environmental, and temperature conditions [169].

Travis Sarver provided a comprehensive review of the impact of dust on the use of solar energy. In the past 20 years, the focus was on the restorative approach. It was primarily washing with water and water/detergent solutions and sometimes, the "automated system" was used for cleaning large systems. The solutions-based systems are very effective, but depend heavily on the availability of quantities of water. Cleaning dirty panels with commercial detergents can be time-consuming, costly, hazardous to the environment, or even corrode the solar

panel frame. Ideally solar panels should be cleaned every few weeks to maintain peak efficiency, which is especially hard to do for large and difficult to reach solar-panel arrays [170].

The dust accumulation problem requires solutions that are adapted to both the intensity of the soiling process and the size of the solar system. For dustier regions or large utility- scale systems, dust accumulation can significantly reduce the capacity of the system. In these cases, cleaning for large installations can run into the range of multi- million dollars per year for fields that are now in the 200- MW size.

7.3. Anti-corrosion

The fabrication of surfaces that repel water is very important for the opportunities in the areas of corrosion inhibition for metal components. Due to their strong water repulsion properties, superhydrophobic coatings are ideal for decreasing the rate of breakdown of the oxide film of metal, and as a result the rate of corrosion of the layer underneath decrease.

Liu et al. (2009) fabricated stable superhydrophobic films with a contact angle of 151° on zinc substrates by a simple immersion method into a methanol solution of hydrolyzed 1H,1H,2H,2H-perfluorooctyltrichlorosilane for 5 days at room temperature followed by annealing at 130°C in air for 1 h. The superhydrophobic film showed an effective corrosion-resistant for the zinc interface when immersed in an aqueous solution of 3% NaCl for up to 29 days. By adding a zinc foil into the 1H, 1H, 2H, 2H perfluorooctyltrichlorosilane/methanol solution which contained silicon or steel, SHS were formed on those silicon and steel surfaces [171, 172].

Zhang et. al. (2008) used the intercalation of laurate anions by ion exchange with ZnAl-(layered double hydroxides)- NO_3 film precursors on a porous anodic alumina/aluminium substrate to fabricate a hierarchical micro/ nano structured superhydrophobic film, which enhance the corrosion resistant of the coat for the underlying aluminium [173].

7.4. Drag reduction

Turbulent flows of a liquid along a surface experience frictional drag, a macroscopic phenomenon that affects the speed and efficiency of marine vessels, the cost of pumping oil through a pipeline, and countless other engineering parameters. The drag arises from shear stress, the rate per unit area of momentum transfer from the flow to the surface. SHS can be fabricated to decrease the drag depending on its highly water repellent property and has the ability to form a thin air film over an underwater surface which prevent the wetting of surface. The air film formed on the surface has the ability to take in air depending on the surface tension of water. In order to reduce frictional drag in ships SHS has been used [3].

8. The stability of SHS

For different applications of SHS, the stable behaviour under different conditions needs to be examined. The stability parameter includes:

- a) Stability in solvents including organic and aqueous, basic and acidic solutions
- b) Thermal stability
- c) Stability against the humidity and UV radiation

Generally, there are main factors responsible for damaging SHS which are: high temperature, low pH, and high chloride concentration [3].

9. Limitations in using SHS

While major developments have taken place in the field of SHS, few commercial products with these properties are still being produced. Some of the important explanations and weaknesses are set out as shown in the following points:

- Cost: Owing to the higher total cost of raw materials or the costly process conditions, most production methods are expensive.
- The stability structure and durability: The SHS requires a stable structure for a long time, which is usually not easy particularly in the case of polymer surfaces due to the resistance between the durability and the stability of the SHS.
- Irregular (non-uniform) coatings: The coatings of low energy materials using different techniques are not fool proof. A major problem is the nonuniform application of the material on the surface.
- Coating Deformation: Typically, SH coatings are thin layers on material surfaces that can be eroded by easy rubbing or localized high-pressure water streams.
- Risks of the health and environmental: Fluorine concentrations that can cause health problems such as teeth and bone loss and damage to the kidney, muscles, and nerves are much of the SHS. During removal, the use of inorganic agents and polymers as non-biodegradable coatings can also pose a risk of environmental pollution.
- Vapour condensation: Though water is repelled by all coated surfaces, water vapour is not repelled. If the coating temperature is lower than the dew point, condensation will happen and the coating will be moistened, greatly damaging its superhydrophobic properties.

10. Challenges of superhydrophobic surface

As mentioned before, most methods to fabricate SHS are based on roughness, and surface is covered by low surface energy material. The following parameters are the most challenging problems of SHS: 1-Thermal stability is an important factor in some applications. Many superhydrophobic coatings are polymer based. Polymers change their surface morphology when the temperature is above the glass transmission temperature, and the polymer starts to melt. At even higher temperature, the polymer structure

even starts to degrade, and superhydrophobicity is decreased.

2-Nano-roughness can be easily destroyed by external force and the adhesion of the coating to the substrate is usually weak. So that, the most challenging problem for a self-cleaning surface is mechanical stability.

3-High transparency is very important in applications of SHS related to window and solar cell. In general, transmittance decreases with increasing roughness, especially if the roughness exceeds the wavelength of light. So, reducing the roughness below a certain value (typically less than 100 nm), to achieve high transparency is another challenge.

4- Impalement in cause of time is a problem for SHS. If the height of the roughness is low, most cases the robustness of the Cassie state is poor [20].

11. Conclusions

In this review, the recent trend in the field of the SHS generation has been described. The basic idea to generate the SHS is by forming a surface asperity with a high apparent contact angle ($> 150^\circ$), low hysteresis in the contact angle ($< 10^\circ$), and low sliding angle. For these SHS, several of the properties have been identified. This analysis article refers to the methods of deposition, actions, and implementation of the SHS. While a significant amount of research has been carried out in this sector, it is still confined to laboratory levels and not extended to real-life applications and consumer products due to the many limitations that researchers need to overcome. Limitations to use and challenges to SHS have been addressed.

12. References

- J. Drelich, E. Chibowski, D. Meng, K. Terpilowski, Hydrophilic and superhydrophilic surfaces and materials, *Soft Matter* 7 (2011) 9804-9828.
- D. Sun, K.F. Böhringer, Self-Cleaning: From Bio-Inspired Surface Modification to MEMS/Microfluidics System Integration, 10(2) (2019).
- A.M.A. Mohamed, A.M. Abdullah, N.A. Younan, Corrosion behavior of superhydrophobic surfaces: A review, *Arabian Journal of Chemistry* 8(6) (2015) 749-765.
- S. Kim, Fabrication of Superhydrophobic Surfaces, *Journal of Adhesion Science and Technology - J ADHES SCI TECHNOL* 22 (2008) 235-250.
- J.T. Woodward, H. Gwin, D.K. Schwartz, Contact Angles on Surfaces with Mesoscopic Chemical Heterogeneity, *Langmuir : the ACS journal of surfaces and colloids* 16(6) (2000) 2957-2961.
- T. Nishino, M. Meguro, K. Nakamae, M. Matsushita, Y. Ueda, The Lowest Surface Free Energy Based on -CF₃ Alignment, *Langmuir : the ACS journal of surfaces and colloids* 15(13) (1999) 4321-4323.
- R.N. Wenzel, RESISTANCE OF SOLID SURFACES TO WETTING BY WATER, *Industrial & Engineering Chemistry* 28(8) (1936) 988-994.
- H. Ogihara, J. Xie, T. Saji, Factors determining wettability of superhydrophobic paper prepared by spraying nanoparticle suspensions, *Colloids and Surfaces A: Physicochemical and Engineering Aspects* 434 (2013) 35-41.
- C. Neinhuis, W. Barthlott, Characterization and Distribution of Water-repellent, Self-cleaning Plant Surfaces, *Annals of Botany* 79(6) (1997) 667-677.
- H. Ensikat, P. Ditsche, C. Neinhuis, W. Barthlott, Superhydrophobicity in perfection: The outstanding properties of the lotus leaf, *Beilstein journal of nanotechnology* 2 (2011) 152-61.
- A. Otten, S. Herminghaus, How Plants Keep Dry: A Physicist's Point of View, *Langmuir : the ACS journal of surfaces and colloids* 20(6) (2004) 2405-2408.
- X. Gao, L. Jiang, Water-Repellent Legs of Water Strider, *Nature* 432 (2004) 36.
- A.B.D. Cassie, S. Baxter, Wettability of porous surfaces, *Transactions of the Faraday Society* 40(0) (1944) 546-551.
- Z. Pan, F. Cheng, B. Zhao, Bio-Inspired Polymeric Structures with Special Wettability and Their Applications: An Overview, *Polymers* 9(12) (2017).
- S. Nishimoto, B. Bhushan, Bioinspired self-cleaning surfaces with superhydrophobicity, superoleophobicity, and superhydrophilicity, *RSC Advances* 3(3) (2013) 671-690.
- Y. Zheng, X. Gao, L. Jiang, Directional adhesion of superhydrophobic butterfly wings, *Soft Matter* 3(2) (2007) 178-182.
- W. Lee, M.K. Jin, W.C. Yoo, J.K. Lee, Nanostructuring of a polymeric substrate with well-defined nanometer-scale topography and tailored surface wettability, *Langmuir : the ACS journal of surfaces and colloids* 20(18) (2004) 7665-9.
- Y. Jung, B. Bhushan, Biomimetic Structures for Fluid Drag Reduction in Laminar and Turbulent Flows, *Journal of physics. Condensed matter : an Institute of Physics journal* 22 (2010) 035104.
- S.-H. Hong, J. Hwang, H. Lee, Replication of cicada wing's nano-patterns by hot embossing and UV nanoimprinting, *Nanotechnology* 20 (2009) 385303.
- M. Eriksson, A. Swerin, Forces at superhydrophobic and superamphiphobic surfaces, *Current Opinion in Colloid & Interface Science* 47 (2020) 46-57.
- B. Bhushan, Y.C. Jung, Natural and biomimetic artificial surfaces for superhydrophobicity, self-cleaning, low adhesion, and drag reduction, *Progress in Materials Science* 56(1) (2011) 1-108.
- M. Nosonovsky, B. Bhushan, Superhydrophobic surfaces and emerging applications: Non-adhesion, energy, green engineering, *Current Opinion in Colloid & Interface Science* 14(4) (2009) 270-280.
- C. Huh, S.G. Mason, Effects of surface roughness on wetting (theoretical), *Journal of Colloid and Interface Science* 60(1) (1977) 11-38.
- X.-M. Li, D. Reinhoudt, M. Crego-Calama, What do we need for a superhydrophobic surface? A review on the recent progress in the preparation of superhydrophobic surfaces, *Chemical Society Reviews* 36(8) (2007) 1350-1368.
- L. Barbieri, E. Wagner, P. Hoffmann, Water Wetting Transition Parameters of Perfluorinated Substrates with Periodically Distributed Flat-Top Microscale Obstacles, *Langmuir : the ACS journal of surfaces and colloids* 23(4) (2007) 1723-1734.
- A. Lafuma, D. Quéré, Superhydrophobic states, *Nature Materials* 2(7) (2003) 457-460.
- Y.C. Jung, B. Bhushan, Dynamic Effects Induced Transition of Droplets on Biomimetic Superhydrophobic Surfaces, *Langmuir : the ACS journal of surfaces and colloids* 25(16) (2009) 9208-9218.
- T. Koishi, K. Yasuoka, S. Fujikawa, T. Ebisuzaki, X.C. Zeng, Coexistence and transition between Cassie and Wenzel state on pillared hydrophobic surface, *Proceedings of the National Academy of Sciences* 106(21) (2009) 8435.
- M. Ma, R.M. Hill, Superhydrophobic surfaces, *Current Opinion in Colloid & Interface Science* 11(4) (2006) 193-202.
- P. Roach, N.J. Shirtcliffe, M.I. Newton, Progress in superhydrophobic surface development, *Soft Matter* 4(2) (2008) 224-240.
- W. Xu, T. Ning, X. Yang, S. Lu, Fabrication of superhydrophobic surfaces on zinc substrates, *Applied Surface Science* 257(11) (2011) 4801-4806.

- [32] Artificial (Biomimetic) Superhydrophobic Surfaces, in: M. Nosonovsky, B. Bhushan (Eds.), *Multiscale Dissipative Mechanisms and Hierarchical Surfaces: Friction, Superhydrophobicity, and Biomimetics*, Springer Berlin Heidelberg, Berlin, Heidelberg, 2008, pp. 199-230.
- [33] M. Mortazavi, Nosonovsky, Michael, Adhesion, Wetting, and Superhydrophobicity of Polymeric Surfaces, 2013.
- [34] D. Ebert, B. Bhushan, Durable Lotus-effect surfaces with hierarchical structure using micro- and nanosized hydrophobic silica particles, *J Colloid Interface Sci* 368(1) (2012) 584-91.
- [35] C.-H. Chang, M.-H. Hsu, C.-J. Weng, W.-I. Hung, T.-L. Chuang, K.-C. Chang, C.-W. Peng, Y.-C. Yen, J.-M. Yeh, 3D-bioprinting approach to fabricate superhydrophobic epoxy/organophilic clay as an advanced anticorrosive coating with the synergistic effect of superhydrophobicity and gas barrier properties, *Journal of Materials Chemistry A* 1(44) (2013) 13869-13877.
- [36] G. Davaasuren, C.-V. Ngo, H.-S. Oh, D.-M. Chun, Geometric study of transparent superhydrophobic surfaces of molded and grid patterned polydimethylsiloxane (PDMS), *Applied Surface Science* 314 (2014) 530-536.
- [37] Y. Qing, Y. Zheng, C. Hu, Y. Wang, Y. He, Y. Gong, Q. Mo, Facile approach in fabricating superhydrophobic ZnO/polystyrene nanocomposite coating, *Applied Surface Science* 285 (2013) 583-587.
- [38] S. Jau-Ye, K. Chun-Wen, C. Peilin, Fabrication of tunable superhydrophobic surfaces, *Proc.SPIE*, 2004.
- [39] F. Palumbo, C. Lo Porto, P. Favia, Plasma Nano-Texturing of Polymers for Wettability Control: Why, What and How, *Coatings* 9(10) (2019).
- [40] J. Zhang, J. Li, Y. Han, Superhydrophobic PTFE Surfaces by Extension, *Macromolecular Rapid Communications* 25(11) (2004) 1105-1108.
- [41] H. Yabu, M. Shimomura, Single-Step Fabrication of Transparent Superhydrophobic Porous Polymer Films, *Chemistry of Materials* 17(21) (2005) 5231-5234.
- [42] X. Lu, C. Zhang, Y. Han, Low-Density Polyethylene Superhydrophobic Surface by Control of Its Crystallization Behavior, *Macromolecular Rapid Communications* 25(18) (2004) 1606-1610.
- [43] L. Jiang, Y. Zhao, J. Zhai, A Lotus-Leaf-like Superhydrophobic Surface: A Porous Microsphere/Nanofiber Composite Film Prepared by Electrohydrodynamics, *Angewandte Chemie International Edition* 43(33) (2004) 4338-4341.
- [44] J. Zhang, X. Lu, W. Huang, Y. Han, Reversible Superhydrophobicity to Superhydrophilicity Transition by Extending and Unloading an Elastic Polyamide Film, *Macromolecular Rapid Communications* 26(6) (2005) 477-480.
- [45] N. Zhao, J. Xu, Q. Xie, L. Weng, X. Guo, X. Zhang, L. Shi, Fabrication of Biomimetic Superhydrophobic Coating with a Micro-Nano-Binary Structure, *Macromolecular Rapid Communications* 26(13) (2005) 1075-1080.
- [46] R. Mohammadi, J. Wassink, A. Amirfazli, Effect of Surfactants on Wetting of Super-Hydrophobic Surfaces, *Langmuir : the ACS journal of surfaces and colloids* 20(22) (2004) 9657-9662.
- [47] H. Yan, K. Kurogi, H. Mayama, K. Tsujii, Environmentally Stable Super Water-Repellent Poly(alkylpyrrole) Films, *Angewandte Chemie International Edition* 44(22) (2005) 3453-3456.
- [48] X. Feng, L. Feng, M. Jin, J. Zhai, L. Jiang, D. Zhu, Reversible Super-hydrophobicity to Super-hydrophilicity Transition of Aligned ZnO Nanorod Films, *Journal of the American Chemical Society* 126(1) (2004) 62-63.
- [49] Y.H. Yang, Z.Y. Li, B. Wang, C. Wang, D. Chen, G. Yang, Self-assembled ZnO agave-like nanowires and anomalous superhydrophobicity, *Journal of Physics: Condensed Matter* 17 (2005) 5441.
- [50] X. Feng, J. Zhai, L. Jiang, The Fabrication and Switchable Superhydrophobicity of TiO₂ Nanorod Films, *Angewandte Chemie (International ed. in English)* 44 (2005) 5115-8.
- [51] S.S. Latthe, A. Gurav, C.S. Maruti, R. Vhatkar, Recent progress in preparation of superhydrophobic surfaces: A review, *J. Surf. Eng. Mater. Adv. Technol.* 2 (2012) 76-94.
- [52] J. Liu, W. Huang, Y. Xing, R. Li, J. Dai, Preparation of durable superhydrophobic surface by sol-gel method with water glass and citric acid, *Journal of Sol-Gel Science and Technology* 58(1) (2011) 18-23.
- [53] A. Roig, E. Molins, E. Rodríguez, S. Martínez, M. Moreno-Mañas, A. Vallribera, Superhydrophobic silica aerogels by fluorination at the gel stage, *Chemical Communications* (20) (2004) 2316-2317.
- [54] H.M. Shang, Y. Wang, S.J. Limmer, T.P. Chou, K. Takahashi, G.Z. Cao, Optically transparent superhydrophobic silica-based films, *Thin Solid Films* 472(1) (2005) 37-43.
- [55] Y. Xiu, D.W. Hess, C.P. Wong, UV and thermally stable superhydrophobic coatings from sol-gel processing, *Journal of Colloid and Interface Science* 326(2) (2008) 465-470.
- [56] P.M. Barkhudarov, P.B. Shah, E.B. Watkins, D.A. Doshi, C.J. Brinker, J. Majewski, Corrosion inhibition using superhydrophobic films, *Corrosion Science* 50(3) (2008) 897-902.
- [57] S.S. Latthe, H. Imai, V. Ganesan, A.V. Rao, Superhydrophobic silica films by sol-gel co-precursor method, *Applied Surface Science* 256(1) (2009) 217-222.
- [58] I. Sas, R. Gorga, J. Joines, K. Thoney-Barletta, Literature review on superhydrophobic self-cleaning surfaces produced by electrospinning, *Journal of Polymer Science B Polymer Physics* 50 (2012) 824-845.
- [59] S.H. Park, S.M. Lee, H.S. Lim, J.T. Han, D.R. Lee, H.S. Shin, Y. Jeong, J. Kim, J.H. Cho, Robust Superhydrophobic Mats based on Electrospun Crystalline Nanofibers Combined with a Silane Precursor, *ACS Applied Materials & Interfaces* 2(3) (2010) 658-662.
- [60] K. Acatay, E. Simsek, C. Ow-Yang, Y.Z. Menceloglu, Tunable, Superhydrophobically Stable Polymeric Surfaces by Electrospinning, *Angewandte Chemie International Edition* 43(39) (2004) 5210-5213.
- [61] M. Ma, R.M. Hill, J.L. Lowery, S.V. Fridrikh, G.C. Rutledge, Electrospun Poly(Styrene-block-dimethylsiloxane) Block Copolymer Fibers Exhibiting Superhydrophobicity, *Langmuir : the ACS journal of surfaces and colloids* 21(12) (2005) 5549-5554.
- [62] M. Kang, R. Jung, H.-S. Kim, H.-J. Jin, Preparation of superhydrophobic polystyrene membranes by electrospinning, *Colloids and Surfaces A: Physicochemical and Engineering Aspects* 313-314 (2008) 411-414.
- [63] X.H. Xu, Z.Z. Zhang, J. Yang, X. Zhu, Study of the corrosion resistance and loading capacity of superhydrophobic meshes fabricated by spraying method, *Colloids and Surfaces A: Physicochemical and Engineering Aspects* 377(1) (2011) 70-75.
- [64] N. Zhao, F. Shi, Z. Wang, X. Zhang, Combining Layer-by-Layer Assembly with Electrodeposition of Silver Aggregates for Fabricating Superhydrophobic Surfaces, *Langmuir : the ACS journal of surfaces and colloids* 21(10) (2005) 4713-4716.
- [65] L. Zhai, F.Ç. Cebeci, R.E. Cohen, M.F. Rubner, Stable Superhydrophobic Coatings from Polyelectrolyte Multilayers, *Nano Letters* 4(7) (2004) 1349-1353.
- [66] S. Amigoni, E. Taffin de Givenchy, M. Dufay, F. Guittard, Covalent Layer-by-Layer Assembled Superhydrophobic Organic-Inorganic Hybrid Films, *Langmuir : the ACS journal of surfaces and colloids* 25(18) (2009) 11073-11077.
- [67] T.T. Isimjan, T. Wang, S. Rohani, A novel method to prepare superhydrophobic, UV resistance and anti-corrosion steel surface, *Chemical Engineering Journal* 210 (2012) 182-187.
- [68] L. Kong, X. Chen, G. Yang, L. Yu, P. Zhang, Preparation and characterization of slice-like Cu₂(OH)₃NO₃ superhydrophobic structure on copper foil, *Applied Surface Science* 254(22) (2008) 7255-7258.
- [69] S. Li, S. Zhang, X. Wang, Fabrication of Superhydrophobic Cellulose-Based Materials through a Solution-Immersion Process, *Langmuir : the ACS journal of surfaces and colloids* 24(10) (2008) 5585-5590.
- [70] C. Dong, Y. Gu, M. Zhong, L. Li, K. Sezer, M. Ma, W. Liu, Fabrication of superhydrophobic Cu surfaces with tunable regular micro and random nano-scale structures by hybrid laser texture and chemical etching, *Journal of Materials Processing Technology* 211(7) (2011) 1234-1240.
- [71] B. Qian, Z. Shen, Fabrication of Superhydrophobic Surfaces by Dislocation-Selective Chemical Etching on Aluminum, Copper, and Zinc Substrates, *Langmuir : the ACS journal of surfaces and colloids* 21(20) (2005) 9007-9009.

- [72] Z. Guo, F. Zhou, J. Hao, W. Liu, Stable Biomimetic Super-Hydrophobic Engineering Materials, *Journal of the American Chemical Society* 127(45) (2005) 15670-15671.
- [73] N.J. Shirtcliffe, G. McHale, M.I. Newton, C.C. Perry, Wetting and Wetting Transitions on Copper-Based Super-Hydrophobic Surfaces, *Langmuir: the ACS journal of surfaces and colloids* 21(3) (2005) 937-943.
- [74] S.M. Li, B. Li, J.H. Liu, M. Yu, Corrosion resistance of superhydrophobic film on aluminum alloy surface fabricated by chemical etching and anodization, *Chinese Journal of Inorganic Chemistry* 28 (2012) 1755-1762.
- [75] K. Teshima, H. Sugimura, Y. Inoue, O. Takai, A. Takano, Transparent ultra water-repellent poly(ethylene terephthalate) substrates fabricated by oxygen plasma treatment and subsequent hydrophobic coating, *Applied Surface Science* 244(1) (2005) 619-622.
- [76] K. Ogawa, M. Soga, Y. Takada, I. Nakayama, Development of a Transparent and Ultrahydrophobic Glass Plate, *Japanese Journal of Applied Physics* 32(Part 2, No. 4B) (1993) L614-L615.
- [77] J. Gao, Y. Li, Y. Li, H. Liu, W. Yang, Fabrication of superhydrophobic surface of stearic acid grafted zinc by using an aqueous plasma etching technique, *Open Chemistry* 10(6) (2012) 1766-1772.
- [78] X. Song, J. Zhai, Y. Wang, L. Jiang, Fabrication of Superhydrophobic Surfaces by Self-Assembly and Their Water-Adhesion Properties, *The Journal of Physical Chemistry B* 109(9) (2005) 4048-4052.
- [79] H. Liu, L. Feng, J. Zhai, L. Jiang, D. Zhu, Reversible wettability of a chemical vapor deposition prepared ZnO film between superhydrophobicity and superhydrophilicity, *Langmuir: the ACS journal of surfaces and colloids* 20(14) (2004) 5659-61.
- [80] L. Zhu, Y. Xiu, J. Xu, P.A. Tamirisa, D.W. Hess, C.-P. Wong, Superhydrophobicity on Two-Tier Rough Surfaces Fabricated by Controlled Growth of Aligned Carbon Nanotube Arrays Coated with Fluorocarbon, *Langmuir: the ACS journal of surfaces and colloids* 21(24) (2005) 11208-11212.
- [81] L. Huang, S.P. Lau, H.Y. Yang, E.S.P. Leong, S.F. Yu, S. Praver, Stable Superhydrophobic Surface via Carbon Nanotubes Coated with a ZnO Thin Film, *The Journal of Physical Chemistry B* 109(16) (2005) 7746-7748.
- [82] C.-T. Hsieh, W.-Y. Chen, F.-L. Wu, Fabrication and superhydrophobicity of fluorinated carbon fabrics with micro/nanoscaled two-tier roughness, *Carbon* 46(9) (2008) 1218-1224.
- [83] X. Zhang, F. Shi, J. Niu, Y. Jiang, Z. Wang, Superhydrophobic surfaces: from structural control to functional application, *Journal of Materials Chemistry* 18(6) (2008) 621-633.
- [84] A.A. Syed, M.K. Dinesan, Review: Polyaniline—A novel polymeric material, *Talanta* 38(8) (1991) 815-837.
- [85] W. Hong-Zhi, Z. Peng, W.-G. Zhang, Y. Su-Wei, Electrodeposition and Characterization of Polyaniline Film, *Chemical Research in Chinese Universities* 28 (2012).
- [86] L. Zhang, Z.D. Zujovic, H. Peng, G.A. Bowmaker, P.A. Kilmartin, J. Travas-Sejdic, Structural Characteristics of Polyaniline Nanotubes Synthesized from Different Buffer Solutions, *Macromolecules* 41(22) (2008) 8877-8884.
- [87] D. Kim, J. Choi, J.-Y. Kim, Y.-K. Han, D. Sohn, Size Control of Polyaniline Nanoparticle by Polymer Surfactant, *Macromolecules* 35(13) (2002) 5314-5316.
- [88] X.-S. Du, C.-F. Zhou, G.-T. Wang, Y.-W. Mai, Novel Solid-State and Template-Free Synthesis of Branched Polyaniline Nanofibers, *Chemistry of Materials* 20(12) (2008) 3806-3808.
- [89] H. Xia, J. Narayanan, D. Cheng, C. Xiao, X. Liu, H.S.O. Chan, Formation of Ordered Arrays of Oriented Polyaniline Nanoparticle Nanorods, *The Journal of Physical Chemistry B* 109(26) (2005) 12677-12684.
- [90] C. Bock, C. Paquet, M. Couillard, G.A. Botton, B.R. MacDougall, Size-Selected Synthesis of PtRu Nano-Catalysts: Reaction and Size Control Mechanism, *Journal of the American Chemical Society* 126(25) (2004) 8028-8037.
- [91] E. Song, J.-W. Choi, Conducting Polyaniline Nanowire and Its Applications in Chemiresistive Sensing, *Nanomaterials (Basel, Switzerland)* 3(3) (2013) 498-523.
- [92] S. Stafström, J.L. Brédas, A.J. Epstein, H.S. Woo, D.B. Tanner, W.S. Huang, A.G. MacDiarmid, Polaron lattice in highly conducting polyaniline: Theoretical and optical studies, *Phys Rev Lett* 59(13) (1987) 1464-1467.
- [93] A.J. Heeger, Semiconducting and Metallic Polymers: The Fourth Generation of Polymeric Materials, *The Journal of Physical Chemistry B* 105(36) (2001) 8475-8491.
- [94] A.G. MacDiarmid, A.J. Epstein, Polyanilines: a novel class of conducting polymers, *Faraday Discussions of the Chemical Society* 88(0) (1989) 317-332.
- [95] A. Ray, A.F. Richter, A.G. MacDiarmid, A.J. Epstein, Polyaniline: protonation/deprotonation of amine and imine sites, *Synthetic Metals* 29(1) (1989) 151-156.
- [96] M. Nechtschein, F. Genoud, C. Menardo, K. Mizoguchi, J.P. Travers, B. Villeret, On the nature of the conducting state of polyaniline, *Synthetic Metals* 29(1) (1989) 211-218.
- [97] P.M. McManus, R.J. Cushman, S.C. Yang, Influence of oxidation and protonation on the electrical conductivity of polyaniline, *The Journal of Physical Chemistry* 91(3) (1987) 744-747.
- [98] T.y.V. Vernitskaya, O.N. Efimov, Polypyrrole: a conducting polymer; its synthesis, properties and applications, *Russian Chemical Reviews* 66(5) (1997) 443-457.
- [99] K.K. Kanazawa, A.F. Diaz, R.H. Geiss, W.D. Gill, J.F. Kwak, J.A. Logan, J.F. Rabolt, G.B. Street, 'Organic metals': polypyrrole, a stable synthetic 'metallic' polymer, *Journal of the Chemical Society, Chemical Communications* (19) (1979) 854-855.
- [100] A.F. Diaz, K.K. Kanazawa, G.P. Gardini, Electrochemical polymerization of pyrrole, *Journal of the Chemical Society, Chemical Communications* (14) (1979) 635-636.
- [101] S. Asavapiriyant, G.K. Chandler, G.A. Gunawardena, D. Pletcher, The electrodeposition of polypyrrole films from aqueous solutions, *Journal of Electroanalytical Chemistry and Interfacial Electrochemistry* 177(1) (1984) 229-244.
- [102] B.R. Scharifker, E. García-Pastoriza, W. Marino, The growth of polypyrrole films on electrodes, *Journal of Electroanalytical Chemistry and Interfacial Electrochemistry* 300(1) (1991) 85-98.
- [103] A.A. Yakovleva, Electrochemistry of Polypyrrole Films in Aqueous Solutions: The Character of the Bond between the Anion and the Polymer Matrix, *Russian Journal of Electrochemistry* 36(12) (2000) 1275-1282.
- [104] M. Yamaura, K. Sato, T. Hagiwara, Effect of counter-anion exchange on electrical conductivity of polypyrrole films, *Synthetic Metals* 41(1) (1991) 439-442.
- [105] B. Grunden, J.O. Iroh, Formation of graphite fibre-polypyrrole coatings by aqueous electrochemical polymerization, *Polymer* 36(3) (1995) 559-563.
- [106] S.P. Armes, Optimum reaction conditions for the polymerization of pyrrole by iron(III) chloride in aqueous solution, *Synthetic Metals* 20(3) (1987) 365-371.
- [107] S. Machida, S. Miyata, A. Techagumpuch, Chemical synthesis of highly electrically conductive polypyrrole, *Synthetic Metals* 31(3) (1989) 311-318.
- [108] L.J. Buckley, D.K. Royle, G.E. Wnek, Influence of dopant ion and synthesis variables on mechanical properties of polypyrrole films, *Journal of Polymer Science Part B: Polymer Physics* 25(10) (1987) 2179-2188.
- [109] P.C. Innis, Y.C. Chen, S. Ashraf, G.G. Wallace, Electrohydrodynamic polymerisation of water-soluble poly((4-(3-pyrrolyl)butane sulfonate), *Polymer* 41(11) (2000) 4065-4076.
- [110] J.M. Pringle, J. Efthimiadis, P.C. Howlett, J. Efthimiadis, D.R. MacFarlane, A.B. Chaplin, S.B. Hall, D.L. Officer, G.G. Wallace, M. Forsyth, Electrochemical synthesis of polypyrrole in ionic liquids, *Polymer* 45(5) (2004) 1447-1453.
- [111] Y. Pornputtkul, L.A.P. Kane-Maguire, G.G. Wallace, Influence of Electrochemical Polymerization Temperature on the Chiroptical Properties of (+)-Camphorsulfonic Acid-Doped Polyaniline, *Macromolecules* 39(17) (2006) 5604-5610.

- [112] G. Inzelt, M. Pineri, J.W. Schultze, M.A. Vorotyntsev, Electron and proton conducting polymers: recent developments and prospects, *Electrochimica Acta* 45(15) (2000) 2403-2421.
- [113] L. Zhang, S. Dong, The electrocatalytic oxidation of ascorbic acid on polyaniline film synthesized in the presence of camphorsulfonic acid, *Journal of Electroanalytical Chemistry* 568 (2004) 189-194.
- [114] M.P. Sokolova, M.A. Smirnov, I.A. Kasatkin, I.Y. Dmitriev, N.N. Saprykina, A.M. Toikka, E. Lahderanta, G.K. Elyashevich, Interaction of Polyaniline with Surface of Carbon Steel, *International Journal of Polymer Science* 2017 (2017) 6904862.
- [115] M.M. Gvozdenovic, B.Z. Jugovic, J.S. Stevanovic, B.N. Grgur, Electrochemical synthesis of electroconducting polymers/Elektrohemijska sinteza elektroprovodnih polimera, *Hemijska Industrija* 68 (2014) 673+.
- [116] M.C. Miras, C. Barbero, O. Haas, Preparation of polyaniline by electrochemical polymerization of aniline in acetonitrile solution, *Synthetic Metals* 43(1) (1991) 3081-3084.
- [117] R. Balint, N.J. Cassidy, S.H. Cartmell, Conductive polymers: Towards a smart biomaterial for tissue engineering, *Acta Biomaterialia* 10(6) (2014) 2341-2353.
- [118] J. Pringle, J. Efthimiadis, P. Howlett, J. Efthimiadis, D. MacFarlane, A. Chaplin, S. Hall, D. Officer, G. Wallace, M. Forsyth, Electrochemical synthesis of polypyrrole in ionic liquids, *Polymer* 45 (2004) 1447-1453.
- [119] S. Mu, Pronounced effect of the ionic liquid on the electrochromic property of the polyaniline film: Color changes in the wide wavelength range, *Electrochimica Acta - ELECTROCHIM ACTA* 52 (2007) 7827-7834.
- [120] Y. Şahin, A. Aydin, Y.A. Udum, K. Pekmez, A. Yıldız, Electrochemical synthesis of sulfonated polypyrrole in FSO₃H/acetonitrile solution, *Journal of Applied Polymer Science* 93(2) (2004) 526-533.
- [121] Y. Şahin, S. Perçin, G.Ö. Alsancak, Electrochemical synthesis of poly(2-iodoaniline) and poly(aniline-co-2-iodoaniline) in acetonitrile, *Journal of Applied Polymer Science* 89(6) (2003) 1652-1658.
- [122] J. Heinze, B.A. Frontana-Uribe, S. Ludwigs, Electrochemistry of Conducting Polymers—Persistent Models and New Concepts, *Chemical Reviews* 110(8) (2010) 4724-4771.
- [123] P.C. Innis, J. Mazurkiewicz, T. Nguyen, G.G. Wallace, D. MacFarlane, Enhanced electrochemical stability of polyaniline in ionic liquids, *Current Applied Physics* 4(2) (2004) 389-393.
- [124] M. Li, C. Ma, B. Liu, Z. Jin, A novel electrolyte 1-ethylimidazolium trifluoroacetate used for electropolymerization of aniline, *Electrochemistry Communications - ELECTROCHEM COMMUN* 7 (2005) 209-212.
- [125] S. Bialozor, A. Kupniewska, Conducting polymers electrodeposited on active metals, *Synthetic Metals* 155(3) (2005) 443-449.
- [126] M.M. Gvozdenović, B.N. Grgur, Electrochemical polymerization and initial corrosion properties of polyaniline-benzoate film on aluminum, *Progress in Organic Coatings* 65(3) (2009) 401-404.
- [127] M.M. Popović, B.N. Grgur, Electrochemical synthesis and corrosion behavior of thin polyaniline-benzoate film on mild steel, *Synthetic Metals* 143(2) (2004) 191-195.
- [128] B.N. Grgur, P. Živković, M.M. Gvozdenović, Kinetics of the mild steel corrosion protection by polypyrrole-oxalate coating in sulfuric acid solution, *Progress in Organic Coatings* 56(2) (2006) 240-247.
- [129] G. Ćirić-Marjanović, Recent advances in polyaniline research: Polymerization mechanisms, structural aspects, properties and applications, *Synthetic Metals* 177 (2013) 1-47.
- [130] J.L. Camalet, J.C. Lacroix, S. Aeiyaich, K. Chane-Ching, P.C. Lacaze, Electrodeposition of protective polyaniline films on mild steel, *Journal of Electroanalytical Chemistry* 416(1) (1996) 179-182.
- [131] J.C. Lacroix, J.L. Camalet, S. Aeiyaich, K.I. Chane-Ching, J. Petitjean, E. Chauveau, P.C. Lacaze, Aniline electropolymerization on mild steel and zinc in a two-step process, *Journal of Electroanalytical Chemistry* 481(1) (2000) 76-81.
- [132] J.L. Camalet, J.C. Lacroix, D. Nguyen, S. Aeiyaich, M.C. Pham, J. Petitjean, P.C. Lacaze, Aniline electropolymerization on platinum and mild steel from neutral aqueous media, *Journal of Electroanalytical Chemistry* 485 (2000) 13-20.
- [133] N.M. Martyak, P. McAndrew, J.E. McCaskie, J. Dijon, Electrochemical polymerization of aniline from an oxalic acid medium, *Progress in Organic Coatings* 45(1) (2002) 23-32.
- [134] J.L. Camalet, J.C. Lacroix, S. Aeiyaich, P.C. Lacaze, Characterization of polyaniline films electrodeposited on mild steel in aqueous p-toluenesulfonic acid solution, *Journal of Electroanalytical Chemistry* 445(1) (1998) 117-124.
- [135] D.L. Wise, *Electrical and Optical Polymer Systems Fundamentals: Methods, and Applications*, CRC Press (1998) 1256.
- [136] V. Gupta, N. Miura, Large-area network of polyaniline nanowires prepared by potentiostatic deposition process, *Electrochemistry Communications* 7(10) (2005) 995-999.
- [137] L. Huang, Z. Wang, H. Wang, X. Cheng, A. Mitra, Y. Yan, Polyaniline nanowires by electropolymerization from liquid crystalline phases, *Journal of Materials Chemistry - J MATER CHEM* 12 (2002) 388-391.
- [138] S. Mu, Y. Yang, Spectral Characteristics of Polyaniline Nanostructures Synthesized by Using Cyclic Voltammetry at Different Scan Rates, *The Journal of Physical Chemistry B* 112(37) (2008) 11558-11563.
- [139] P. Nunziante, G. Pistoia, Factors affecting the growth of thick polyaniline films by the cyclic voltammetry technique, *Electrochimica Acta* 34(2) (1989) 223-228.
- [140] Y. Zhou, M. Freitag, J. Hone, C. Staii, A.T. Johnson, N.J. Pinto, A.G. MacDiarmid, Fabrication and electrical characterization of polyaniline-based nanofibers with diameter below 30 nm, *Applied Physics Letters* 83(18) (2003) 3800-3802.
- [141] Z.-M. Huang, Y.Z. Zhang, M. Kotaki, S. Ramakrishna, A review on polymer nanofibers by electrospinning and their applications in nanocomposites, *Composites Science and Technology* 63(15) (2003) 2223-2253.
- [142] J. Wang, Y.L. Bunimovich, G. Sui, S. Savvas, J. Wang, Y. Guo, J.R. Heath, H.-R. Tseng, Electrochemical fabrication of conducting polymer nanowires in an integrated microfluidic system, *Chemical Communications* (29) (2006) 3075-3077.
- [143] D.H.C. Reneker, Iksoo, Nanometre diameter fibres of polymer, produced by electrospinning, *Nanotechnology* 7 (Issue 3) (1996) pp. 216-223
- [144] R. Córdova, M.A. del Valle, A. Arratia, H. Gómez, R. Schrebler, Effect of anions on the nucleation and growth mechanism of polyaniline, *Journal of Electroanalytical Chemistry* 377(1) (1994) 75-83.
- [145] W. Dhaoui, M. Bouzitoun, H. Zarrouk, H.B. Ouada, A. Pron, Electrochemical sensor for nitrite determination based on thin films of sulfamic acid doped polyaniline deposited on Si/SiO₂ structures in electrolyte/insulator/semiconductor (E.I.S.) configuration, *Synthetic Metals* 158(17) (2008) 722-726.
- [146] K. Kozieł, M. Łapkowski, Studies on the influence of the synthesis parameters on the doping process of polyaniline, *Synthetic Metals* 55(2) (1993) 1011-1016.
- [147] A. Pron, P. Rannou, Processible conjugated polymers: from organic semiconductors to organic metals and superconductors, *Progress in Polymer Science* 27(1) (2002) 135-190.
- [148] H. Okamoto, T. Kotaka, Structure and properties of polyaniline films prepared via electrochemical polymerization. I: Effect of pH in electrochemical polymerization media on the primary structure and acid dissociation constant of product polyaniline films, *Polymer* 39(18) (1998) 4349-4358.
- [149] S. Pruneanu, E. Csahók, V. Kertész, G. Inzelt, Electrochemical quartz crystal microbalance study of the influence of the solution composition on the behaviour of poly(aniline) electrodes, *Electrochimica Acta* 43(16) (1998) 2305-2323.
- [150] G. Zotti, S. Cattarin, N. Comisso, Cyclic potential sweep electropolymerization of aniline: The role of anions in the polymerization mechanism, *Journal of Electroanalytical Chemistry and Interfacial Electrochemistry* 239(1) (1988) 387-396.
- [151] P. Fedorko, M. Trznadel, A. Pron, D. Djurado, J. Planès, J.P. Travers, New analytical approach to the insulator-metal transition in conductive polyaniline, *Synthetic Metals* 160(15) (2010) 1668-1671.

- [152] N.V. Blinova, J. Stejskal, M. Trchová, J. Prokeš, M. Omastová, Polyaniline and polypyrrole: A comparative study of the preparation, *European Polymer Journal* 43(6) (2007) 2331-2341.
- [153] G. Inzelt, *Conducting Polymers*, (2012).
- [154] S. Mu, C. Chen, J. Wang, The kinetic behavior for the electrochemical polymerization of aniline in aqueous solution, *Synthetic Metals* 88(3) (1997) 249-254.
- [155] T.P.D. Krzysztof Matyjaszewski, *HANDBOOK OF RADICAL POLYMERIZATION*, (2002).
- [156] B.-S. Kim, W.H. Kim, S.N. Hoier, S.-M. Park, Electrochemistry of conductive polymers XVI. Growth mechanism of polypyrrole studied by kinetic and spectroelectrochemical measurements, *Synthetic Metals* 69(1) (1995) 455-458.
- [157] F. Beck, M. Oberst, R. Jansen, On the mechanism of the filmforming electropolymerization of pyrrole in acetonitrile with water, *Electrochimica Acta* 35(11) (1990) 1841-1848.
- [158] R.L. Townsin, The Ship Hull Fouling Penalty, *Biofouling* 19(sup1) (2003) 9-15.
- [159] C.S. Gudipati, J.A. Finlay, J.A. Callow, M.E. Callow, K.L. Wooley, The antifouling and fouling-release performance of hyperbranched fluoropolymer (HBFP)-poly(ethylene glycol) (PEG) composite coatings evaluated by adsorption of biomacromolecules and the green fouling alga *Ulva*, *Langmuir: the ACS journal of surfaces and colloids* 21(7) (2005) 3044-53.
- [160] H. Zhang, R. Lamb, J. Lewis, Engineering nanoscale roughness on hydrophobic surface—preliminary assessment of fouling behaviour, *Science and Technology of Advanced Materials* 6(3) (2005) 236-239.
- [161] O.-U. Nimitrakoolchai, S. Supothina, Deposition of organic-based superhydrophobic films for anti-adhesion and self-cleaning applications, *Journal of the European Ceramic Society* 28(5) (2008) 947-952.
- [162] C.-H. Xue, S.-T. Jia, J. Zhang, J.-Z. Ma, Large-area fabrication of superhydrophobic surfaces for practical applications: an overview, *Science and Technology of Advanced Materials* 11(3) (2010) 033002.
- [163] F. Mejia, J. Kleissl, J.L. Bosch, The Effect of Dust on Solar Photovoltaic Systems, *Energy Procedia* 49 (2014) 2370-2376.
- [164] A.M. El-Nashar, Effect of dust deposition on the performance of a solar desalination plant operating in an arid desert area, *Solar Energy* 75(5) (2003) 421-431.
- [165] A. Salim, F. Huraib, N.N. Eugenio, *PV power-study of system options and optimization*, 1988.
- [166] H.K. Elminir, A.E. Ghitas, R.H. Hamid, F. El-Hussainy, M.M. Beheary, K.M. Abdel-Moneim, Effect of dust on the transparent cover of solar collectors, *Energy Conversion and Management* 47(18) (2006) 3192-3203.
- [167] M.S. El-Shobokshy, F.M. Hussein, Degradation of photovoltaic cell performance due to dust deposition on to its surface, *Renewable Energy* 3(6) (1993) 585-590.
- [168] S.A.M. Said, Effects of dust accumulation on performances of thermal and photovoltaic flat-plate collectors, *Applied Energy* 37(1) (1990) 73-84.
- [169] M. Mani, R. Pillai, Impact of dust on solar photovoltaic (PV) performance: Research status, challenges and recommendations, *Renewable and Sustainable Energy Reviews* 14(9) (2010) 3124-3131.
- [170] T. Sarver, A. Al-Qaraghuli, L.L. Kazmerski, A comprehensive review of the impact of dust on the use of solar energy: History, investigations, results, literature, and mitigation approaches, *Renewable and Sustainable Energy Reviews* 22 (2013) 698-733.
- [171] H. Liu, S. Szunerits, W. Xu, R. Boukherroub, Preparation of Superhydrophobic Coatings on Zinc as Effective Corrosion Barriers, *ACS Applied Materials & Interfaces* 1(6) (2009) 1150-1153.
- [172] H. Liu, S. Szunerits, M. Pisarek, W. Xu, R. Boukherroub, Preparation of Superhydrophobic Coatings on Zinc, Silicon, and Steel by a Solution-Immersion Technique, *ACS applied materials & interfaces* 1 (2009) 2086-91.
- [173] F. Zhang, L. Zhao, H. Chen, S. Xu, D.G. Evans, X. Duan, Corrosion Resistance of Superhydrophobic Layered Double Hydroxide Films on Aluminum, *Angewandte Chemie International Edition* 47(13) (2008) 2466-2469.